Title: Genomic effects of the glucocorticoid receptor guide the acute stress-induced delayed anxiety and basolateral amygdala spine plasticity in rats

Running Title: GCs, NOR, and the delayed effects of acute stress

Leonardo Santana Novaes[1], Leticia Morais Bueno-de-Camargo[1], Amadeu Shigeo de Almeida[1], Vitor Augusto Laurino Juliano[1], Nilton Barreto dos Santos[1†], Ki Ann Goosens[2], Carolina Demarchi Munhoz[1*].

Affiliation: [1]Department of Pharmacology, Universidade de Sao Paulo Instituto de Ciencias Biomedicas, São Paulo, Brazil, 05508-000.

†*In memorian.*

[2]Department of Psychiatry, Icahn School of Medicine at Mount Sinai, New York, NY 10029

*__Corresponding author__: Carolina Demarchi Munhoz at Department of Pharmacology, Av. Professor Lineu Prestes, 1524, room 323. Universidade de Sao Paulo Instituto de Ciencias Biomedicas, São Paulo - SP, 05508-000, Brazil. Phone Number: + 55 11 3091 7990.

Email: cdmunhoz@usp.br

Abstract

Anxiety, a state related to anticipatory fear, can be adaptive in the face of environmental threats or stressors. However, anxiety can also become persistent and manifest as anxiety- and stress-related disorders, such as generalized anxiety or post-traumatic stress disorder (PTSD). In rodents, systemic administration of glucocorticoids (GCs) or short-term restraint stress induces anxiety-like behaviors and dendritic branching within the basolateral complex of the amygdala (BLA) ten days later. Additionally, increased arousal-related memory retention mediated by elevated GCs requires concomitant noradrenaline (NE) signaling, both acting in the BLA. It is unknown whether GCs and NE play a role in the delayed acute stress effects on BLA dendritic plasticity and behavior. Here, we show that inhibiting corticosterone (CORT) elevation during the two-hour restraint stress prevents stress-induced increases in delayed anxiety-like behaviors and BLA dendritic spine density in rats. Also, we show that acute stress's behavioral and morphological delayed effects are critically dependent on glucocorticoid receptor (GR) genomic actions in the BLA. Unlike CORT, the pharmacological enhancement of NE signaling in the BLA was insufficient to drive delayed anxiety-related behavior. Nonetheless, the delayed anxiety-like behavior 10 days after acute stress requires NE signaling in the BLA at the time it is expressed. Therefore, we define essential roles for two stress-related hormones acting at two different times, for the late stress consequences: CORT, via GR, immediately at stress; NE, via beta-adrenoceptors, during the expression of delayed behavior.

Significance Statement

The dysregulation in orchestrating and finetuning major stress-related neural circuitries leads to enhanced reactivity and other altered ways of coping with threatening situations. These predispose humans to multiple psychiatric disorders, including anxiety and PTSD. Given the tremendous burden of affective disorders, we must advance our understanding of stress neurobiology and translate this into improved treatments. Here we showed that the absence of neuronal GR genomic signaling in the BLA prevented delayed effects on dendritic spine density and anxiety-like behavior ten days after stressor exposure. We also define essential roles for two stress-related hormones acting at two different times, for the late stress consequences: CORT, via GR, immediately at stress; NE, via beta-adrenoceptors, during the expression of delayed behavior.

Keywords: stress; neuroplasticity; amygdala; glucocorticoid signaling; anxiety; behavior.

Introduction

The body's physiological and behavioral responses to stressful stimuli have critical adaptive value as it prepares to deal with threatening conditions. The almost immediate release of norepinephrine (NE) in the brain during emotional arousal binds to alpha and beta-adrenergic receptors (1). Tens of minutes later, the release of glucocorticoid hormones (GCs) reaches a peak; GCs drive many acute adaptations to stress through actions at glucocorticoid receptors (GRs) [for a review, (2)]. A seminal work showed that elevation of corticosterone (CORT; the principal GC in rodents) enhances memory retention in tasks with high arousal content (3). Interestingly, the authors showed that arousal is set by the NE levels that reach the amygdala's basolateral complex (BLA) (3).

However, maladaptation can sometimes follow stressor exposure (4). Exacerbated fear responses to stimuli that would not usually elicit such a response, avoidance behavior, and persistent anxiety symptoms are characteristic of anxiety- and stress-related disorders, such as generalized anxiety disorder and post-traumatic stress disorder (PTSD) (5). The relationship between an acute stressor and the delayed manifestation of anxiety symptoms has been widely studied, mainly because it resembles stress-related psychiatric disorders, including PTSD.

Several studies have shown that a single two-hour stress session is sufficient to generate anxiety-like behavior ten days later (6-9). Also, both two-hour restraint stress and the single prolonged stress protocols, in addition to promoting delayed anxiety-related behavior in rats, are associated with deficits in fear extinction memory (10, 11).

Some studies have shown that either acute two-hour immobilization stress or a systemic elevation of CORT promotes, 10 to 12 days later, anxiety-like behavior in rats accompanied by increased spine density and dendritic arborization in rats BLA (7, 12, 13). This delayed effect of stress on behavior is associated with morphological changes in the BLA, suggesting that increased synaptic contacts in this brain area are the basis for the increased anxiogenic drive. Hyperexcitability of the amygdala has also been linked to anxiety (14). Thus, it seems logical that hypertrophy of BLA dendritic trees plays a causal role in anxiety.

Although there is a clear relationship between a transient increase in CORT levels and emergent anxiety-related behavior, it is unclear whether CORT acts directly upon BLA neurons to cause behavioral and morphological dendritic plasticity effects after an acute

87 episode of stress. It also remains to be clarified whether these morphological changes in the
88 BLA are sufficient to promote anxiety or if there is a dependence on another mediator, in
89 addition to CORT, for the delayed behavioral manifestation associated with acute stress.
90 Thus, in this work, we sought to better understand the role of GR, particularly the genomic
91 actions of this receptor, in the BLA at the time of stress in stress-induced behavioral and
92 morphological outcomes. Also, considering the arousal-inducing effect of catecholamines
93 and their modulation on neuronal excitability (15), we explored the role of the adrenergic
94 receptors in the BLA in expressing stress-induced anxiety-related behavior.

95 **Materials and Methods**

96 ***Subjects***

97 Male Wistar rats (60-days old) were obtained from either the Facility for SPF Rat
98 Production at the Institute of Biomedical Sciences - Animal Facility Network at the
99 University of São Paulo (USP) or Harlan Sprague-Dawley (United States) and maintained in
100 the vivarium of the USP Pharmacology Department (Unit 1) or Massachusetts Institute of
101 Technology (MIT). Neonatal Wistars rats (1 to 4 days old) were used for the cortical
102 primary culture. Upon arrival, the animals were pair-housed in standard polypropylene
103 cages (30 X 40 X 18 cm) with ad libitum access to food and water, kept in a 12-hour light-
104 dark cycle (light on at 6:00 am), and under controlled temperature (23 ± 2 ºC). All
105 experiments were conducted under the standards of the Ethics Committee for Animal Use of
106 the Institute of Biomedical Sciences/University of São Paulo (CEUA - ICB 85/2016) and by
107 the Committee for Animal Care at MIT. All methods were in accordance with the Guidelines
108 of the Brazilian National Council for the Control of Animal Experimentation (CONCEA) and
109 the US National Institutes of Health (NIH) Guide for the Care and Use of Laboratory Animals.

110 ***Animal experimental procedures***

111 *Acute restraint stress*

112 The animals were placed in a ventilated PVC restraint tube for 2 hours in a lighted and
113 soundproof room. The behavioral experiments were conducted 10 days after the end of the
114 stress session.

115 *Behavioral tests*

The behavioral tests were conducted in a room of soundproof and low light (10-14 lux). All tests were videotaped using a digital video camera (Logitech C920, Lausanne, Switzerland) from the top of the apparatuses. After each session, the apparatuses were cleaned with 5% alcohol to remove olfactory cues.

Elevated plus maze

Animals were placed in the center of the maze (elevation of 50 cm, 50 cm × 10 cm each arm), facing one of the open arms, and allowed to freely explore the apparatus for 5 min. We scored entries, time spent in each arm, and the total displacement in the maze using Ethovision software (Noldus, the Netherlands). Anxiety index (16, 17) was calculated as follows: 1 - [(time spent in open arms/total time on the maze) + (number of entries to the open arms/Total exploration on the maze)/2].

Light/dark box

Animals were placed in the middle of the light chamber (45 x 41 x 21 cm light chamber, 65 lx; 35 x 41 x 21 cm dark chamber, 0 lx) facing the opposite side of the connecting door. Each trial lasted 5 min, and the duration of time spent in the light chamber was used as a parameter to address anxiety-like behavior.

Stereotactic surgery

Drugs and viral vectors were injected into the BLA through stereotaxic surgery as described by (18), with some modifications. Rats were anesthetized with Isoflurane (4% oxygen saturation for induction and 2-3% for maintenance), received a dose of anti-inflammatory for preventive analgesia (ketoprofen, 5 mg/kg, subcutaneous), and were set up in the stereotaxic instrument (Kopf Instruments). After disinfection of the skin (70% ethanol, 1% iodine, and 2% glycerin), the skin covering the skull was incised, and small holes were drilled in the skull surface for the passage of cannulae or injection needles. The stainless-steel guide cannulae (23-gauge, World Precision Instruments) were positioned bilaterally 1.0 mm dorsal to the BLA, as the following coordinates: A/P, -2.4; M/L, ± 5.1; D/V, -6.0 mm relative to bregma and the surface of the brain (19). The cannulae were fixed with polyacrylic cement and anchored to the skull with stainless steel screws. Drug infusions were made through injectors (30-gauge stainless steel that extended 1.0mm beyond the tip of each guide cannula) after the animal's complete recovery from cannula implantation

146 surgery (4 to 5 days). The injectors were connected to a Hamilton syringe (5 µl, Hamilton
147 Co., Reno, NV) through a polypropylene tube, and the infusion rate was 0.1µl/min with 1
148 min for diffusion before the injector was removed from the guide cannula. The viral
149 particles were injected with the aid of stainless-steel needles coupled to a Hamilton syringe
150 (5 µl, Hamilton Co, Reno, NV) fixed in an infusion pump (Pump 11 Elite, Harvard Apparatus)
151 coupled to the stereotaxic apparatus. The injections were placed bilaterally in the BLA,
152 following the coordinates: A/P, -2.4; M/L, ± 5.1; D/V, -7.0 mm. The viruses were infused at a
153 rate of 0.1µl/min for 20 min (total of 2µl per injection site, totaling 2 X 106 viral particles).
154 The needles remained in place for 10 minutes before being removed. The injections were
155 performed 4-5 days before stress, a critical time to reach the viral expression peak 5. Only
156 animals with bilateral viral infection in the BLA were considered in the behavioral analysis.
157 After surgery, the animals were under observation for 3 days, and if they showed any sign of
158 pain or discomfort, they received a daily dose of anti-inflammatory (ketoprofen, 5 mg/kg,
159 subcutaneous).

160 *Cannula placement verification, viral infection visualization, and immunofluorescence*

161 Cannula placement verification was done by Nissl staining. The expression of GFP indicated
162 viral infection into BLA. Animals in which the cannulae were not correctly positioned
163 bilaterally on the BLA, i.e., GFP expression was not restricted to the BLA, were excluded
164 from the study. The GFP detection and immunofluorescence assay are detailed below.

165 ***Drug administration***

166 Metyrapone (i.p.; 150 mg in 1 ml of saline; Sigma-Aldrich) was administered 1.5 hours
167 before restraint stress. Bilateral intra-BLA infusion of RU-486 (10ng in 0.5 µl of 5% DMSO;
168 Sigma-Aldrich), dexamethasone (30 ng in 1 µl of 0.5% ethanol), propranolol (2.5 µg in 0.5 µl
169 of saline), or yohimbine (2.5 µg in 0.5 µl of saline), or their corresponding vehicle controls,
170 were also performed.

171 ***Viral vector construct***

172 Viral vectors containing the dnGR receptor gene sequence were constructed as previously
173 described (20-22). The dnGR gene construct is a chimera composed of the rat GR alpha
174 subunit (Genbank M14053), containing the ligand-binding domain, fused to the human GR
175 beta subunit (Genbank X03348), which contains the DNA-binding site domain. The viral

176 construct was obtained from the MIT viral core facility (McGovern Institute, MIT). dnGR was
177 packaged in the HSV p1005 vector (short-term expression), a Herpes Simplex Virus 1 (HSV-
178 1) derived amplicon plasmid with an added transcription cassette expressing GFP (separate
179 promoter and poly(A)) (23, 24). The empty vector (lacking the dnGR sequence) was used as
180 a control. The target gene is driven by the IE 4/5 promoter, while a CMV promoter drives
181 the GFP. The two transcription cassettes are in a nose-to-tail orientation. Adherent 2.2 cells
182 were transfected with the plasmid of interest (containing dnGR). The transfection was done
183 using the Lipofectamine LTX reagent (Invitrogen). Twenty-four hours after transfection, the
184 cells were super-infected with Helper Virus 5dl1.2, with a multiplicity of infection = 0.03.
185 The cells and media were harvested 48 hours later when the virus's cytopathic effect
186 reached 100%. The solutions were frozen and thawed three times, sonicated to release
187 infectious viral particles, and then centrifuged to clear the media of cell debris. The resulting
188 supernatant passed onto 2-2 cells. This amplification procedure was repeated twice. After
189 the final sonication and centrifugation, the supernatant was purified on a sucrose gradient,
190 viral bands were centrifuged, and viral pellets were resuspended in 10% sucrose in D-PBST.
191 The vector titration was quantified in Vero cells by counting the cells expressing the GFP
192 protein. An average titration of approximately 1 x 106 viral particles per µl was achieved.

193 ***Dendritic spine density analysis***

194 For some experiments, the brains were prepared using the Rapid Golgi Kit (FD
195 NeuroTechnologies, Inc.) according to the manufacturer's instructions. An
196 immunohistochemistry assay was performed for other experiments to amplify the GFP
197 signal to analyze the dendritic spine density in the BLA neurons previously infected with
198 the HSV vector. Brains were incubated in impregnation solution for 14 days followed by
199 incubation in cryoprotectant solution for 48 h, coronally sliced (120 µm) using a Leica
200 CM3050-S cryostat (Leica Biosystems) and mounted on gelatin-coated slides. Brain sections
201 were dehydrated in ethanol, diaphonized in xylene, and coverslipped. The BLA images were
202 captured in a bright field with the slide scanner Zeiss Axio Scan.Z1 (Zeiss), using a 40X
203 objective. A z-stack was created with a step size of 410 nm, and the images were analyzed in
204 ZEN 2 (Zeiss) software with a magnification of 600×. At least 5 neurons per animal (4
205 animals per group) were analyzed according to the following criteria: only neurons with the
206 soma wholly localized in the BLA, heavily impregnated, without truncated dendrites. After
207 neuronal soma identification, we classified each dendritic segment as primary (originating

208 from the soma), secondary (originating from the primary branch), tertiary (originating from
209 the secondary branch), or quaternary (originating from the tertiary branch). Regardless of
210 the morphologic classification, all protrusions originating from a dendrite were considered
211 spines. After we determined the origin and the end of each branch, the dendritic branch
212 length was calculated by the software.

213 ***Brain tissue processing for immunofluorescence and immunohistochemistry***

214 Brains were sectioned in a cryostat (Leica CM3050-S, Leica Biosystems, Germany) in a
215 coronal plane (40-µm-thick) at -22 °C and stored in an anti-freeze solution (0.05 M sodium
216 phosphate buffer, 150 g of sucrose, and 300 ml of ethylene glycol) at -20 °C.

217 We performed the immunofluorescence assay to visualize GR expression in the BLA. Brain
218 slices were incubated in blocking solution (0.02 M potassium phosphate solution containing
219 0.3% X-100 triton and 1% bovine albumin) for 1 hour, followed by incubation in blocking
220 solution containing the primary antibody (rabbit anti-GR, dilution 1: 1000, Santa Cruz;
221 mouse anti-MAP-2, dilution 1: 5000, Sigma-Aldrich) for 18h (4 °C). The slices were then
222 incubated for 2h (room temperature) in a 0.02M potassium phosphate solution containing
223 the secondary donkey antibody conjugated to a fluorochrome (AlexaFluor 594 anti-rabbit,
224 dilution 1: 500, Thermo Fisher Scientific; AlexaFluor 488 anti-mouse, dilution 1: 500,
225 Thermo Fisher Scientific). Brain slices were mounted on positively charged slides
226 (Fisherbrand Superfroast Plus, Thermo Fisher Scientific) and covered with a coverslip using
227 Fluoromount-G as a mounting medium (SouthernBiotech). The images were acquired in a
228 confocal microscope (Nikon A1R +, Nikon Instruments Inc., Japan), sectioned in the Z plane
229 at 0.6 µm.

230 Although the HSV vector carries the gene that encodes GFP, an immunohistochemistry
231 procedure was performed to intensify the signal and improve GFP particles' detection
232 throughout the BLA dendritic tree. Brain slices were incubated in blocking solution (0.02 M
233 potassium phosphate solution containing 0.3% X-100 triton and 3% normal donkey serum)
234 followed by incubation in blocking solution containing the primary antibody anti-GFP
235 raised in rabbit (dilution 1: 1000; Thermo Fisher Scientific) for 18 hours (4 °C). The slices
236 were then incubated in a 0.02 M potassium phosphate solution containing a biotinylated
237 donkey antibody (dilution 1: 200; Vector) and 0.3% X-100 triton for 2 h at room
238 temperature. The antigen-antibody complex was visualized with the biotin-avidin technique

239 (Elite kit; Vector) and 3,3'-diaminobenzidine (DAB) as a chromogen through a peroxidase
240 reaction composed of a 2.5% solution of nickel sulfate and 0.003% hydrogen peroxide in
241 0.02M potassium phosphate buffer. The sections were mounted on gelatin-coated slides,
242 air-dried, and dipped in a 0.05% aqueous solution of osmium tetroxide for 20 s to enhance
243 the labeling's visibility, dehydrated, transferred into xylene, and coverslipped with DPX.
244 Spine density was quantified under a bright field, as detailed for the Golgi staining assay.

245 **Western Blot**

246 The GR expression and its phosphorylated form were analyzed by western blot as
247 previously (17).

248 *Protein extraction*

249 Cytosolic and nuclear protein extracts were obtained using the Cel-LyticTM NuCLEARTM
250 Extraction Kit (Sigma–Aldrich Co.). BLA tissues stored at -80 ºC were thawed and
251 mechanically homogenized with a conical plastic pestle (Thermo Fisher Scientific) in cold
252 lysis buffer (10 mM HEPES, pH 7.9, 10 mM KCl, 1.5 mM MgCl2, 0.5 mm PMSF, 1 mm DTT)
253 supplemented with protease and phosphatase inhibitors (Halt Protease Inhibitor Cocktail,
254 ThermoFisher Scientific), and centrifuged for 20 min at 11,000xg at 4 °C. The supernatant
255 (cytosolic fraction) was collected in a tube and stored at -80 °C. The remaining pellets were
256 homogenized in the extraction buffer (20 mM HEPES, pH 7.9, 300 mM NaCl, 1.5 mM MgCl2,
257 0.25 mM EDTA, 0.5 mM PMSF, 0.5 mM DTT 25% glycerol) supplemented with protease and
258 phosphatase inhibitors, kept on ice for 30 min, and centrifuged for 5 min at 20,000xg (4 °C).
259 The resulting supernatants (nuclear proteins) were stored at -80 °C. Protein concentration
260 was determined using the Bradford method (Bio-Rad Laboratories, Inc).

261 *Electrophoresis*

262 Protein samples (20 µg/lane) were size-separated in 10% SDS-PAGE gel (90 V) and then
263 blotted onto Immobilon® PVDF membrane (EMD Millipore Corporation). The Ponceau
264 method for immunoblot was used to ensure equal protein loading (25). Blots were blocked
265 with 5% bovine serum albumin (BSA) diluted in TBS-T buffer (50 mM Tris-HCl, 150 mM
266 NaCl, 0.1% Tween 20, pH 7.5) for 1 h at room temperature and subsequently incubated
267 overnight at 4 °C with specific primary antibodies: monoclonal rabbit anti-GR (dilution
268 1:1000, Santa Cruz) and polyclonal rabbit anti-Ser211phospho-GR (dilution 1:1000, Cell

269 Signaling). After incubation with the primary antibodies, the membrane was then probed
270 with a secondary antibody conjugated to horseradish peroxidase (dilution of 1:2000,
271 Kirkegaard & Perry Laboratories) for 2 h at room temperature, and the signal was obtained
272 by the Luminata Forte Western HRP substrate (Merck Millipore, Darmstadt, Germany)
273 using the ChemiDoc system (Bio-Rad Laboratories). Several exposure times were
274 performed to ensure the linearity of the band intensities. Each band's relative density was
275 normalized to the value of α-Tubulin (sc-5286, dilution: 1:20,000, Santa Cruz
276 Biotechnology).

277 **Primary cortical cell culture**

278 Neonatal rats, between 1 and 4 days post-natal, were sacrificed by decapitation, and then
279 the frontal cortex was dissected in a sterile medium (Hanks buffer: 160 mM NaCl, 5.3 mM
280 KCl, 0.44 Kh2PO4, 0.33 mM Na2HPO4, 5.5 mM glucose, 4.0 mM NaHCO3) supplemented
281 with antibiotics (penicillin/streptomycin, Invitrogen), at pH 7.4. The isolated frontal cortex
282 was maintained in Hanks buffer containing 0.05% trypsin solution (Vitrocell) and 0.001%
283 DNAse (Sigma-Aldrich) at 37 °C for 10 minutes and then transferred to Dulbecco's Modified
284 Eagle Medium culture medium (DMEN; Vitrocel) supplemented with 10% fetal bovine
285 serum (FBS, Vitrocel) and 2 mM glutamine (Sigma-Aldrich). The suspension was gently
286 mechanically grounded with the aid of a Pasteur pipette. The solution was filtered through a
287 70 µM membrane (Becton-Dickinson), and the cells were further cultured in a 24-well plate
288 and maintained at 37 °C with 5% CO2 in a humidified atmosphere (80% relative humidity)
289 in an incubator. For immunofluorescence assay, cells were cultured on borosilicate
290 coverslips covered with poly-L-lysine (0.01%, Sigma-Aldrich) in a 24-well plate. To
291 calculate the number of viral particles necessary for efficient infection, the number of cells
292 was counted before plating using the Trypan Blue exclusion method (Sigma-Aldrich, MO,
293 USA). The cells were maintained in DMEN supplemented with antibiotics and 10% SFB. The
294 medium was changed on the second and fifth days after culturing, and the cells were
295 maintained until the tenth day.

296 *Infection of cells by viral particles and analysis of sub-localization and genomic activity of GR*

297 To check the sublocalization of the dnGR receptor in the cell compartments, in response to
298 CORT, culture cells were infected with the viral particles (HSV-dnGR and HSV-GFP, MOI of
299 1) diluted in culture medium (DMEN + 2% SFB) on the eighth culture day. Forty-eight hours

300 later (tenth day of culture), the cells were treated with 10 µM CORT in the culture medium
301 (DMEN + 2% SFB) for 1h. Then, the medium was removed, and the coverslips were washed
302 with PBS and then fixed with 4% formaldehyde (Amresco) for 20 minutes at room
303 temperature. After 5 washes with PBS, the cells adhered to the coverslips were incubated in
304 the blocking solution (5% donkey serum, 0.05% Triton X-100 in PBS) for 2h at room
305 temperature. Subsequently, the cells were incubated in a blocking solution containing the
306 primary anti-GR antibody (1: 1000, Santa Cruz) for 24 hours and then, after washing with
307 PBS, incubated in PBS containing the secondary antibody (AlexaFluor 594, 1: 2000) and
308 0.05% Triton X-100 for 2h. Finally, the coverslips were incubated in DAPI solution (1:
309 100000, Sigma-Aldrich; PBS with 0.05% Triton X-100) for 20 minutes, washed with PBS,
310 and mounted on slides in Fluoromount-G mounting medium (SouthernBiotech, USA). The
311 slides were analyzed under a fluorescence microscope (Nikon Eclipse 80i; Nikon
312 Instruments Inc., Japan).

313 For the analysis of GR genomic activity in cells infected by tdGR, the polymerase chain
314 reaction (PCR) assay was performed to amplify the *gilz* and *fkbp5* genes described below.
315 The cells were obtained using the same protocol for image analysis, but the cells were
316 cultured on 6-well plates. At the end of the treatment with CORT, the cells were washed 5
317 times with PBS and collected in TRIzol® (0.75 µl per sample; Thermo Fisher Scientific).
318 RNA extraction followed the manufacturer's instructions.

319 *Polymerase chain reaction (PCR)*

320 The cDNA was obtained using the SuperScript III Reverse Transcriptase Kit (Thermo Fisher
321 Scientific) according to the manufacturer's instructions. For the reaction, 12 µl of final
322 solution were used, containing 5 µg of RNA, 1 µl of dNTPs (0.5nM each), 1 µl of Random
323 Primer, and 5 µg of total RNA in sterile water.

324 For the amplification, 2 µl of the cDNA (20 ng / µl), 5 µl of Amp Buffer, 0.75 ul MgCl2, 0.5 µl
325 of dNTPs, 1.5 µl of the forward primer, 1.5 µl of the reverse primer, 0.5 µl of Taq Polymerase
326 (Promega Co), and Milli-Q water (Merck Millipore) sufficient for 25 µl were added in a
327 microtube. The reaction conditions in the thermal cycler (LifeECO, Bulldog Bio, Inc) were:
328 95 ° C for 2 initial minutes, followed by 30 cycles at 95 ° C for 1 minute, 55 ° C for 30
329 seconds, and 72 ° C for 1 minute. After the last cycle, the samples remained for 5 minutes at
330 72 ° C. The product was separated using agarose gel electrophoresis (2%), stained with

331 BlueGreen (Thermo Fisher Scientific), and visualized with a UV transilluminator (ChemiDoc
332 Imager; Bio-Rad Laboratories, Inc). The sequences of the primers used are as follows:

333 gapdh: forward, 5'-GGTGTGAACGGATTTGGC-3'; reverse, 5'-CTGG-AAGATGGTGATGGGTT-3';

334 gilz: forward, 5'-TGGGGCCTAGTAACACCAAG-3'; reverse, 5'-GAGCACACTGGCATCACATC-3'

335 fkbp5: forward, 5'-GAACCCAATGCTGAGCTTATG-3'; reverse, 5'-
336 ATGTACTTGCCTCCCTTGAAG-3'.

337 **Euthanasia of the animals and obtaining the analyzed material**

338 *Guillotine beheading, BLA dissection, and blood collection*

339 The animals were deeply anesthetized with Isoflurane (maximum exposure of the 30s) and
340 euthanatized by decapitation. The brain was quickly removed in a cold solution of saline-
341 phosphate buffer (137 mM NaCl, 2.68 mM KCl, 1.27 mM KH2PO4, 8.06 mM Na2HPO4). The
342 BLA was bilaterally dissected on a cold glass plate and frozen in a conical tube (1.5 ml) on
343 dry ice. The brain structures were stored at –80 ºC for later use. Brains were placed in a 1
344 mm thick coronal cut acrylic brain matrix (Zivic Laboratories Inc.), and the dissection was
345 performed under a stereomicroscope (Tecnival - Prolab). The animals' blood was obtained
346 from the animal's trunk at the time of decapitation.

347 *Transcardiac perfusion*

348 The animals were deeply anesthetized with a solution of ketamine hydrochloride (9 mg /
349 100 g, i.p.) and xylazine (1 mg / 100g, i.p.) and infused transcardiacally using a peristaltic
350 pump (Cole Parmer), with 200 ml of 0.9% saline followed by about 500 ml of 4%
351 formaldehyde solution in sodium phosphate buffer (pH 7.4) at 4 ° C for 20 minutes. After 3
352 hours, the brain was removed from the skull and kept in a 30% sucrose solution in
353 potassium phosphate buffer (0.02M) at 4 ° C for 48 hours. After this cryoprotection period,
354 the brain was removed from the sucrose solution and frozen at -80 ° C until histological
355 processing.

356 ***Blood collection***

357 Blood was sampled from the body trunk after decapitation, immediately after stress
358 termination. Plasma was obtained by adding EDTA (4.5 mM) to the collected blood and
359 centrifugation at 4,000 g for 10 minutes. Samples were stored at -80 ºC.

360 ***Analysis of the concentration of corticosterone in the blood***

361 We used the Corticosterone EIA kit (Enzo Life Sciences, Inc) to analyze blood CORT levels,
362 following the manufacturer's guidelines. Plasma samples were diluted 30 times in the assay
363 buffer provided by the kit to fit the standard curve's optimal range. The values depicted in
364 the figures were corrected for the dilution factor.

365 ***Statistical analysis***

366 Statistical analysis was performed using two-way ANOVA. Post hoc Tukey's multiple
367 comparison test examined differences between individual groups. Unpaired Student's t-test
368 was used to compare two experimental groups. Sample size and animal numbers were
369 estimated based on previous studies, and outlier samples were checked by the ROUT
370 method. Quantification of data was blind for all experiments. GraphPad Prism software 9.0
371 was used for the statistical analysis, and the level of statistical significance was $p < 0.05$.
372 Data are presented as mean ± SEM. Detailed statistical information for each test performed
373 is reported in the figures.

374 **Results**

375 ***Systemic CORT release is necessary for the delayed stress-induced anxiety-like***
376 ***behavior and increased BLA dendritic spine density.***

377 To confirm whether the acute elevation of CORT plasma levels is essential to these stress-
378 related behavioral and neuroplastic effects, we inhibited the stress-induced rise in this
379 hormone's blood levels by administering metyrapone (Met). This compound inhibits the
380 synthesis of GCs, before stress exposure. We assessed the behavioral outcomes ten days
381 later (Fig. 1*A*). As shown in Fig. 1*B*, pre-stress Met administration effectively prevented the
382 acute stress-induced increase in CORT plasma levels measured immediately after stress
383 exposure, as the stressed animals administered with saline presented higher plasma CORT
384 concentrations than non-stressed animals ($P < 0.001$) or stressed animals treated with Met
385 ($P < 0.001$).

386 Ten days after restraint stress, we assessed the anxiety-like behavior on an elevated plus-
387 maze test (EPM). Likewise, pre-stress Met administration effectively blunted the occurrence
388 of stress-induced anxiety-like behavior. Met-administered stressed animals presented
389 higher open arms exploration than saline-treated stressed animals ($P < 0.01$, Fig. 1*C*; $P <$

390 0.05, Fig. 1*D*) and the same exploration profile as the saline non-stressed animals (Fig. 1*C*
391 and *D*). The anxiety index confirmed these data, being higher in saline stressed animals than
392 in non-stressed ($P < 0.01$) and Met-treated stressed animals ($P < 0.01$) (Fig. 1*E*). Finally,
393 neither stress nor Met treatment influenced the animals' motor behavior, indicated by the
394 maze's total displacement (Fig. 1*F* and *G*).

395 Next, we analyzed the effects of pre-stress Met administration on the delayed stress-
396 induced increase in dendritic spine density in the BLA using Golgi staining in a subset of the
397 rats that underwent behavioral testing (n = 4/group). We confirmed that a single 2-hr
398 restraint stress exposure augmented the spine density in the primary ($P < 0.001$, Fig. 2*A*),
399 secondary ($P < 0.001$, Fig. 2*B*), tertiary ($P < 0.001$, Fig. 2*C*), and quaternary ($P < 0.01$, Fig.
400 2*D*) segments of the BLA dendritic neurons compared to the non-stressed animals. Met
401 administration blunted the stress-induced increase in dendritic spine density in the BLA
402 with no effects in non-stressed animals in all dendritic segments (Fig. 2), suggesting a
403 coordinated role of stress-induced systemic CORT elevation at the time of stress exposure in
404 both BLA neuroplasticity and the late development of anxiety-like behavior.

405 ***The delayed effects of acute stress on anxiety-like behavior and BLA dendritic spine***
406 ***density increase depend on GR's neuronal genomic activity.***

407 Next, we examined whether neuronal GR activation in BLA was implicated in the late stress
408 outcomes associated with acute stress-induced plasma CORT elevation. Two hours of
409 restraint stress increased GR nuclear translocation into BLA neurons immediately after
410 stress (Fig. S1A and *B*), and Western blot analysis revealed not only an increase in GR
411 nuclear translocation in the BLA ($P = 0.0346$; Fig. S1*C*) but also in the phosphorylation at the
412 Ser211 site ($P = 0.0166$; Fig. S1*D*), known to be associated with a gain in GR transcriptional
413 function (26, 27). Notably, ten days after stress and immediately after the EPM test, there
414 was no difference in the GR nuclear translocation in the BLA of the stressed animals (Fig.
415 S2). Likewise, in a previous study, we found no changes in serum CORT levels of animals
416 submitted to EPM previously stressed 10 days before (8).

417 These findings collectively suggest that CORT signaling through GR at the time of stress
418 ultimately triggers delayed changes in the BLA. In line with this, animals infused with the
419 GR antagonist RU486 directly into the BLA immediately prior to stress (Fig. S3*A*) showed,
420 ten days later, a higher percentage of entries ($P = 0.0161$, Fig. S3*B*) and time spent ($P =$

421 0.0215; Fig. S3*C*) in the EPM open arms, with no changes in the total distance traveled in the
422 maze (Fig. S3*D*), when compared to stressed animals that received vehicle infusions.

423 A rise in CORT serum levels leads, via GR, to rapid (non-genomic) and long-lasting
424 (genomic) changes in the BLA neuronal excitability and synaptic plasticity (28, 29). Because
425 of the delayed effect of stress-associated GR signaling on anxiety-like behavior and
426 remodeling of dendritic spines in the BLA, we expressed a transcriptionally inactive,
427 truncated form of GR in the BLA, the so-called dominant negative GR (dnGR). Cultured cells
428 infected with dnGR responded to CORT treatment with the receptor's translocation to the
429 cell nucleus as control GFP-infected cells (Fig. S4*A* and *B*). However, even with a high GR
430 expression in the nucleus, dnGR-infected cells expressed fewer GR-related mRNA
431 transcription products when compared to GFP-infected cells (Fig. S4*C*).

432 The HSV-based plasmid has a peak of transgene expression three to four days after
433 infection, with a subsequent rapid decline in transgene expression (20). Thus, we applied
434 restraint stress four to five days after intra-cranial delivery of the virus (Fig. 3*A*) to
435 maximize any inhibition of GR genomic activity during the stress session. Notably, the
436 behavioral test was administered ten days later, a time point at which viral expression of
437 the transgene should be minimal. Stressed GFP-infected animals exhibited anxiety-like
438 behavior, as shown by reduced entries ($P < 0.01$; Fig. 3*B*) and time spent ($P < 0.01$; Fig. 3*C*)
439 in open arms compared to the GFP non-stressed animals. On the other hand, the expression
440 of dnGR in the BLA prevented the anxiogenic effect of acute stress. These animals, even
441 when stressed, displayed similar levels of open arm exploration compared to the GFP non-
442 stressed and significantly elevated open arm exploration relative to the GFP stressed
443 animals. This situation was observed for open arm entries ($P < 0.05$) and the anxiety index
444 ($P < 0.05$) (Fig. 3*B* and *D*). There were no effects of stress, and dnGR expression on distance
445 traveled in the maze, suggesting differences in motor activity did not contribute to the
446 behavioral difference (Fig. 3*E* and *F*).

447 Additionally, dnGR expression did not impact the release of CORT during acute stress:
448 similar stress-induced levels of CORT were observed in dnGR-Stress and GFP-stress groups
449 (Fig 3*G)* ($P < 0.001$ and $P < 0.01$, respectively) and exhibited similar hormone levels relative
450 to each other. Thus, the blunting of the delayed behavioral consequences of stress by dnGR
451 is not due to altered CORT release.

452 To determine whether dnGR expression also prevented stress-induced changes in BLA
453 spine density, we explored the GFP protein signal throughout all subcellular compartments
454 in brain sections taken from the animals after the EPM and performed the analysis of spine
455 density. Fig. 4 shows a stress-induced increase in the dendritic spine density in animals
456 previously infected with the GFP control construct, compared to non-stressed animals, in
457 the primary ($P < 0.05$; Fig. 4*A*), secondary ($P < 0.05$; Fig. 4*B*), and tertiary ($P < 0.001$; Fig. 4*C*)
458 dendritic segments. The overexpression of dnGR in the BLA prevented the stress-induced
459 increase in the density of spines in the secondary ($P < 0.05$; Fig. 4*B*) and tertiary ($P < 0.001$;
460 Fig. 4*C*) but not in the primary (Fig. 4*A*), dendritic segments.

461 ***An increase in GR activity in the BLA is sufficient to induce a delayed anxiogenic***
462 ***effect***

463 To test whether acute elevation of CORT in the BLA was sufficient to induce delayed anxiety,
464 we stereotaxically injected dexamethasone (Dex) into the BLA and, ten days later, tested the
465 anxiety-related behavior (Fig. S5A). The EPM test showed that Dex infusion lowered the
466 percentage of open-arms entries ($P = 0.0482$; Fig. S5*B*) and time spent in the open arms ($P =$
467 0.0285; Fig. S5*C*), and elevated anxiety index ($P = 0.0127$; Fig. S5*D*), compared to saline-
468 infused stressed animals. We performed a second anxiety-related behavioral test since the
469 Dex-treated animals moved less in the maze than the saline ones ($P = 0.0048$; Fig. S5*E* and
470 *F*). Using the light/dark box test, we confirmed that Dex-treated animals displayed more
471 remarkable anxiety-like behavior than saline-treated animals since Dex-treated animals
472 spent less time in the light compartment than saline-administered animals ($P = 0.0369$; Fig.
473 S5*G*).

474 ***BLA beta-adrenergic receptor activation is necessary for the expression of delayed***
475 ***stress-related anxiety-like behavior***

476 The acute anxiogenic effect of NE is widely known and involves the noradrenergic
477 projections from locus coeruleus (LC) to BLA (30). However, it is not known whether NE
478 has delayed anxiogenic effects. We next addressed this question by infusing the alpha-2
479 adrenergic receptor antagonist yohimbine into the BLA and examining the acute and
480 delayed effects of this manipulation on anxiety-like behavior (Fig. S6A). Antagonizing alpha-
481 2 autoreceptors in the BLA results in increased firing from noradrenergic nerve terminals
482 (12, 13). Consistent with previous reports, we observed that increased activity of NE in BLA

483 had an acute anxiogenic effect in the open field test (Fig S6*B, C, D, E*). In contrast with CORT,
484 intra-BLA administration of yohimbine was insufficient to induce anxiety-like behavior in
485 the EPM test ten days later (Fig. S6*F, G, H, I*).

486 Because increasing NE activity in the BLA has an acute, but not delayed, anxiogenic effect,
487 we next wanted to examine whether beta-adrenergic receptor activity is critical for the
488 delayed manifestation of anxiety-like behavior in previously stressed animals. Thus, we
489 administered saline or propranolol, a beta-adrenoceptor antagonist, into the BLA of the
490 animals before the behavioral test, 10 days after the stress (Fig. 5*A*). As shown in Fig. 5,
491 stressed propranolol-treated animals presented a higher percentage of entries ($P < 0.05$;
492 Fig. 5*B*) and time spent ($P < 0.05$; Fig. 5C) in the EPM than stressed saline-administered
493 animals. These effects were not accompanied by changes in the animals' locomotor activity
494 (Fig. 5*D*). Therefore, these results suggest that even at a delayed time point at which stress-
495 dependent increases in spine density are present (Fig. 2), stress-related changes in anxiety
496 still depend on the activation of beta-receptors in the BLA during the behavioral task.

497 **Discussion**

498 Here, we report that inhibition of CORT synthesis during acute stress prevented stress-
499 related behavioral and morphological effects that emerged after ten days. This finding
500 complements a previous study reporting that single systemic administration of CORT,
501 simulating an acute stress exposure, induced a delayed anxiogenic effect, along with parallel
502 increases in dendritic length, branch points, and spine density in BLA neurons (12, 13). It is
503 important to note that we showed that inhibiting CORT alone (Fig. 1-2), but not
504 catecholamines (Fig. 5, S6), was sufficient to hinder these effects of stress. Together with
505 previous reports in the literature (12, 31), in this study, we have shown that CORT release is
506 essential for the late effects of stress on anxiety-like behavior and dendritic remodeling of
507 the BLA.

508 Amygdala hyperactivity is considered a biological substrate of stress- and anxiety-related
509 disorders in human and animal models (32). Stimulation of BLA projection neurons triggers
510 anxiety-like behavior in rodents (33), while acute and chronic stress increases the intrinsic
511 excitability of BLA pyramidal neurons (34, 35). Likewise, symptoms of anxiety manifested
512 by patients suffering from stress-related disorders, such as PTSD, are correlated with
513 amygdala hyperactivity (36, 37). The greater concentration of synaptic contacts in dendritic

514 spines, compared to the rest of the neuronal surface, confers heightened ionic conductance
515 in this area, leading to a higher probability of evoked excitatory postsynaptic potentials
516 [EPSPs, see (38)]. Likely, delayed morphological changes in the BLA dendritic tree following
517 acute restraint stress produce a more excitable neuronal phenotype, although this remains
518 untested. Accordingly, the delayed anxiogenic effect of single prolonged stress seen in rats
519 co-occurs with hypertrophy in the BLA dendritic tree and increased miniature excitatory
520 and inhibitory postsynaptic frequency currents in this brain area (39). Curiously, in the
521 present study, the lack of GR genomic signaling in the BLA neurons prevented the stress-
522 related increase in the spine density in the most distal dendritic branches (Fig. 4B, C)
523 without affecting the most proximal ones (Fig. 4A). This effect is consistent with other
524 reports that distal synaptic inputs on BLA neurons are more likely to be excitatory. In
525 contrast, proximal synapses are more likely to be inhibitory (40).

526 Acute elevations in blood CORT levels have a modulatory action on the turnover of dendritic
527 spines in the cortex, producing a short-term effect on the elimination and formation of new
528 dendritic spines (41). Interestingly, acute stress and a single systematic injection of CORT
529 promote delayed (at least 10 days later) but not short-term (1 day later) changes in the BLA
530 dendritic tree (7, 31).

531 Protein synthesis is a critical step for the formation of new spines (42), and our findings not
532 only showed that the stress-related anxiety-like behavior and the increase in the BLA
533 dendritic spine density are both governed by the direct action of CORT in this brain region,
534 but that they are phenomena dependent on GR genomic activity. The GR mobilization by
535 dexamethasone injection into BLA generated a delayed anxiety-like behavior even without
536 stress. The mechanism by which GR influences the origin and stabilization of new spines is
537 not yet fully understood. However, growing evidence has shown a synergistic and
538 interdependent action between GR and the TRKB-BDNF receptor in the motor cortex during
539 motor-related learning (43-45).

540 The role of NE in modulating behavior is well known and is closely related to the immediate
541 effects on changing/increasing the perception of threats under a stress exposure (46). Acute
542 stress leads to a rapid release of NE in the limbic system, including BLA and hippocampus,
543 primarily via projections of noradrenergic neurons from the LC (30, 47). The activation of
544 beta-adrenergic receptors in the BLA promotes increased excitatory synaptic transmission

545 and increased neuronal spike firing rates [see (15)]. In the present study, we confirmed an
546 acute anxiogenic effect of increased availability of NE in the BLA (via yohimbine
547 administration) (Fig. S6), but this increase in NE release was insufficient to promote
548 delayed behavioral changes. In contrast, Dex administration in the BLA was sufficient to
549 promote delayed behavioral changes (Fig. S5). Furthermore, blocking NE signaling directly
550 into BLA with propranolol at the time of behavioral testing prevented the anxious-like
551 manifestation in previously stressed animals (Fig. 7).

552 The synergism of GR and noradrenergic transmission in the BLA has already been critical in
553 potentiating the effects of arousal on memory retention (48). Here, we reported a non-
554 simultaneous but coordinated and (possibly) non-direct dependence of the delayed
555 manifestation of stress-induced anxiety on both GR and beta-adrenoceptor signaling in the
556 BLA. It is important to note that previously we did not see any increase in CORT release ten
557 days after the stress and immediately after the EPM test (8), suggesting no role for elevated
558 CORT in the expression of anxiety-like behavior. Thus, we propose that the stress-related
559 delayed plastic changes in the BLA's dendritic arbor depend on GR signaling, and these
560 changes may potentiate the stress response to NE. Therefore, given the morphological
561 effects of stress, the delayed behavioral outcome depends on NE signaling via beta-
562 adrenoceptors.

Acknowledgments

We gratefully thank Guiomar Wiesel for her technical assistance.

Funding

This work was supported by the Fundação de Amparo à Pesquisa do Estado de São Paulo (FAPESP 2016/03572-3 and 2019/00908-9) and Conselho Nacional de Desenvolvimento Científico e Tecnológico (CNPq 422523/2016-0) to CDM and a grant from the US Army Research Office and the Defense Advanced Research Projects Agency (grant W911NF-10-1-0059) to KAG. LSN was supported by FAPESP (2012/24002-0 and 2018/19599-3). LMBC was supported by CAPES, CNPq (142260/2019-3), and FAPESP (2018/15982-7). NBS was supported by FAPESP (2018/17991-3). ASA was supported by FAPESP (2019/00400-5 and 2021/12488-4) and CAPES. VALJ was supported by FAPESP (2020/06914-8 and 2021/13524-4) and CNPq (PIBIC 2019-1429). C.D.M. is a research fellow from CNPq. This study was financed in part by the Coordenação de Aperfeiçoamento de Pessoal de Nível Superior - Brasil (CAPES) - Finance Code 001.

Competing Interest Statement

The authors declared no conflicts of interest concerning their authorship or the publication of this article.

Author Contributions:

LSN: designed research, performed research, analyzed data, wrote the paper; LMBC: performed research, analyzed data; ASA: performed research, analyzed data; NBS: performed research, analyzed data; KAG: designed research, contributed unpublished reagents/analytic tools, wrote the paper; CDM: designed research, analyzed data, contributed unpublished reagents/analytic tools, wrote the paper.

References

1. H. J. Krugers, H. Karst, M. Joels, Interactions between noradrenaline and corticosteroids in the brain: from electrical activity to cognitive performance. *Front Cell Neurosci* **6**, 15 (2012).
2. E. R. de Kloet, M. Joels, F. Holsboer, Stress and the brain: from adaptation to disease. *Nature reviews. Neuroscience* **6**, 463-475 (2005).

3. B. Roozendaal, S. Okuda, E. A. Van der Zee, J. L. McGaugh, Glucocorticoid enhancement of memory requires arousal-induced noradrenergic activation in the basolateral amygdala. *Proceedings of the National Academy of Sciences of the United States of America* **103**, 6741-6746 (2006).
4. B. S. McEwen, H. Akil, Revisiting the Stress Concept: Implications for Affective Disorders. *The Journal of neuroscience : the official journal of the Society for Neuroscience* **40**, 12-21 (2020).
5. D. A. Regier, E. A. Kuhl, D. J. Kupfer, The DSM-5: Classification and criteria changes. *World Psychiatry* **12**, 92-98 (2013).
6. P. Chakraborty, S. Datta, B. S. McEwen, S. Chattarji, Corticosterone after acute stress prevents the delayed effects on the amygdala. *Neuropsychopharmacology : official publication of the American College of Neuropsychopharmacology* **45**, 2139-2146 (2020).
7. R. Mitra, S. Jadhav, B. S. McEwen, A. Vyas, S. Chattarji, Stress duration modulates the spatiotemporal patterns of spine formation in the basolateral amygdala. *Proceedings of the National Academy of Sciences of the United States of America* **102**, 9371-9376 (2005).
8. L. S. Novaes, N. B. Dos Santos, J. G. Perfetto, K. A. Goosens, C. D. Munhoz, Environmental enrichment prevents acute restraint stress-induced anxiety-related behavior but not changes in basolateral amygdala spine density. *Psychoneuroendocrinology* **98**, 6-10 (2018).
9. F. Yasmin *et al.*, Stress-induced modulation of endocannabinoid signaling leads to delayed strengthening of synaptic connectivity in the amygdala. *Proceedings of the National Academy of Sciences of the United States of America* **117**, 650-655 (2020).
10. P. R. Abdullahi *et al.*, Protective effects of morphine in a rat model of post-traumatic stress disorder: Role of hypothalamic-pituitary-adrenal axis and beta- adrenergic system. *Behavioural brain research* **395**, 112867 (2020).
11. L. S. Novaes, L. M. Bueno-de-Camargo, C. D. Munhoz, Environmental enrichment prevents the late effect of acute stress-induced fear extinction deficit: the role of hippocampal AMPA-GluA1 phosphorylation. *Transl Psychiatry* **11**, 18 (2021).
12. R. Mitra, R. M. Sapolsky, Acute corticosterone treatment is sufficient to induce anxiety and amygdaloid dendritic hypertrophy. *Proceedings of the National Academy of Sciences of the United States of America* **105**, 5573-5578 (2008).
13. R. P. Rao, S. Anilkumar, B. S. McEwen, S. Chattarji, Glucocorticoids protect against the delayed behavioral and cellular effects of acute stress on the amygdala. *Biological psychiatry* **72**, 466-475 (2012).
14. N. Daviu, M. R. Bruchas, B. Moghaddam, C. Sandi, A. Beyeler, Neurobiological links between stress and anxiety. *Neurobiol Stress* **11**, 100191 (2019).
15. A. E. Fink, J. E. LeDoux, beta-Adrenergic enhancement of neuronal excitability in the lateral amygdala is developmentally gated. *J Neurophysiol* **119**, 1658-1664 (2018).
16. H. Cohen, M. A. Matar, D. Buskila, Z. Kaplan, J. Zohar, Early post-stressor intervention with high-dose corticosterone attenuates posttraumatic stress response in an animal model of posttraumatic stress disorder. *Biological psychiatry* **64**, 708-717 (2008).
17. L. S. Novaes *et al.*, Environmental enrichment protects against stress-induced anxiety: Role of glucocorticoid receptor, ERK, and CREB signaling in the basolateral amygdala. *Neuropharmacology* **113**, 457-466 (2017).

640 18. L. S. Novaes, S. J. Shammah-Lagnado, Projections from the anteroventral part of the
641 medial amygdaloid nucleus in the rat. *Brain research* **1421**, 30-43 (2011).
642 19. G. Paxinos, C. Watson, *The Rat Brain in Stereotaxic Coordinates.* (Elsevier, London,
643 ed. 6th Edition, 2007), pp. 476.
644 20. D. Kaufer *et al.*, Restructuring the neuronal stress response with anti-glucocorticoid
645 gene delivery. *Nature neuroscience* **7**, 947-953 (2004).
646 21. E. D. Kirby *et al.*, Basolateral amygdala regulation of adult hippocampal
647 neurogenesis and fear-related activation of newborn neurons. *Molecular psychiatry*
648 **17**, 527-536 (2012).
649 22. R. M. Meyer, A. Burgos-Robles, E. Liu, S. S. Correia, K. A. Goosens, A ghrelin-growth
650 hormone axis drives stress-induced vulnerability to enhanced fear. *Molecular*
651 *psychiatry* **19**, 1284-1294 (2014).
652 23. R. L. Neve, F. Lim, Generation of high-titer defective HSV-1 vectors. *Current protocols*
653 *in neuroscience / editorial board, Jacqueline N. Crawley ... [et al.]* **Chapter 4**, Unit 4 13
654 (2013).
655 24. S. J. Russo *et al.*, Nuclear factor kappa B signaling regulates neuronal morphology
656 and cocaine reward. *The Journal of neuroscience : the official journal of the Society for*
657 *Neuroscience* **29**, 3529-3537 (2009).
658 25. O. Salinovich, R. C. Montelaro, Reversible staining and peptide mapping of proteins
659 transferred to nitrocellulose after separation by sodium dodecylsulfate-
660 polyacrylamide gel electrophoresis. *Analytical biochemistry* **156**, 341-347 (1986).
661 26. W. Chen *et al.*, Glucocorticoid receptor phosphorylation differentially affects target
662 gene expression. *Mol Endocrinol* **22**, 1754-1766 (2008).
663 27. M. D. Krstic, I. Rogatsky, K. R. Yamamoto, M. J. Garabedian, Mitogen-activated and
664 cyclin-dependent protein kinases selectively and differentially modulate
665 transcriptional enhancement by the glucocorticoid receptor. *Mol Cell Biol* **17**, 3947-
666 3954 (1997).
667 28. S. Duvarci, D. Pare, Glucocorticoids enhance the excitability of principal basolateral
668 amygdala neurons. *The Journal of neuroscience : the official journal of the Society for*
669 *Neuroscience* **27**, 4482-4491 (2007).
670 29. H. Karst, S. Berger, G. Erdmann, G. Schutz, M. Joels, Metaplasticity of amygdalar
671 responses to the stress hormone corticosterone. *Proceedings of the National*
672 *Academy of Sciences of the United States of America* **107**, 14449-14454 (2010).
673 30. J. G. McCall *et al.*, Locus coeruleus to basolateral amygdala noradrenergic projections
674 promote anxiety-like behavior. *Elife* **6** (2017).
675 31. H. Kim *et al.*, Regional differences in acute corticosterone-induced dendritic
676 remodeling in the rat brain and their behavioral consequences. *BMC Neurosci* **15**, 65
677 (2014).
678 32. B. M. Sharp, Basolateral amygdala and stress-induced hyperexcitability affect
679 motivated behaviors and addiction. *Transl Psychiatry* **7**, e1194 (2017).
680 33. G. G. Calhoon, K. M. Tye, Resolving the neural circuits of anxiety. *Nature neuroscience*
681 **18**, 1394-1404 (2015).
682 34. A. Hetzel, J. A. Rosenkranz, Distinct effects of repeated restraint stress on basolateral
683 amygdala neuronal membrane properties in resilient adolescent and adult rats.
684 *Neuropsychopharmacology : official publication of the American College of*
685 *Neuropsychopharmacology* **39**, 2114-2130 (2014).
686 35. J. A. Rosenkranz, E. R. Venheim, M. Padival, Chronic stress causes amygdala
687 hyperexcitability in rodents. *Biological psychiatry* **67**, 1128-1136 (2010).

688 36. A. M. Hull, Neuroimaging findings in post-traumatic stress disorder. Systematic
689 review. *Br J Psychiatry* **181**, 102-110 (2002).
690 37. R. K. Pitman *et al.*, Biological studies of post-traumatic stress disorder. *Nature*
691 *reviews. Neuroscience* **13**, 769-787 (2012).
692 38. A. T. Gulledge, N. T. Carnevale, G. J. Stuart, Electrical advantages of dendritic spines.
693 *PloS one* **7**, e36007 (2012).
694 39. H. H. Zhang *et al.*, Traumatic Stress Produces Delayed Alterations of Synaptic
695 Plasticity in Basolateral Amygdala. *Front Psychol* **10**, 2394 (2019).
696 40. P. M. Klenowski *et al.*, Structural and functional characterization of dendritic arbors
697 and GABAergic synaptic inputs on interneurons and principal cells in the rat
698 basolateral amygdala. *J Neurophysiol* **114**, 942-957 (2015).
699 41. C. Liston, W. B. Gan, Glucocorticoids are critical regulators of dendritic spine
700 development and plasticity in vivo. *Proceedings of the National Academy of Sciences*
701 *of the United States of America* **108**, 16074-16079 (2011).
702 42. J. Tanaka *et al.*, Protein synthesis and neurotrophin-dependent structural plasticity
703 of single dendritic spines. *Science* **319**, 1683-1687 (2008).
704 43. M. Arango-Lievano *et al.*, Persistence of learning-induced synapses depends on
705 neurotrophic priming of glucocorticoid receptors. *Proceedings of the National*
706 *Academy of Sciences of the United States of America* **116**, 13097-13106 (2019).
707 44. M. Arango-Lievano *et al.*, Neurotrophic-priming of glucocorticoid receptor signaling
708 is essential for neuronal plasticity to stress and antidepressant treatment.
709 *Proceedings of the National Academy of Sciences of the United States of America* **112**,
710 15737-15742 (2015).
711 45. F. Jeanneteau, M. J. Garabedian, M. V. Chao, Activation of Trk neurotrophin receptors
712 by glucocorticoids provides a neuroprotective effect. *Proceedings of the National*
713 *Academy of Sciences of the United States of America* **105**, 4862-4867 (2008).
714 46. G. Aston-Jones, J. Rajkowski, J. Cohen, Role of locus coeruleus in attention and
715 behavioral flexibility. *Biological psychiatry* **46**, 1309-1320 (1999).
716 47. R. J. Valentino, E. Van Bockstaele, Convergent regulation of locus coeruleus activity
717 as an adaptive response to stress. *European journal of pharmacology* **583**, 194-203
718 (2008).
719 48. D. de Quervain, L. Schwabe, B. Roozendaal, Stress, glucocorticoids and memory:
720 implications for treating fear-related disorders. *Nature reviews. Neuroscience* **18**, 7-
721 19 (2017).

722

723 **Figures and Tables**

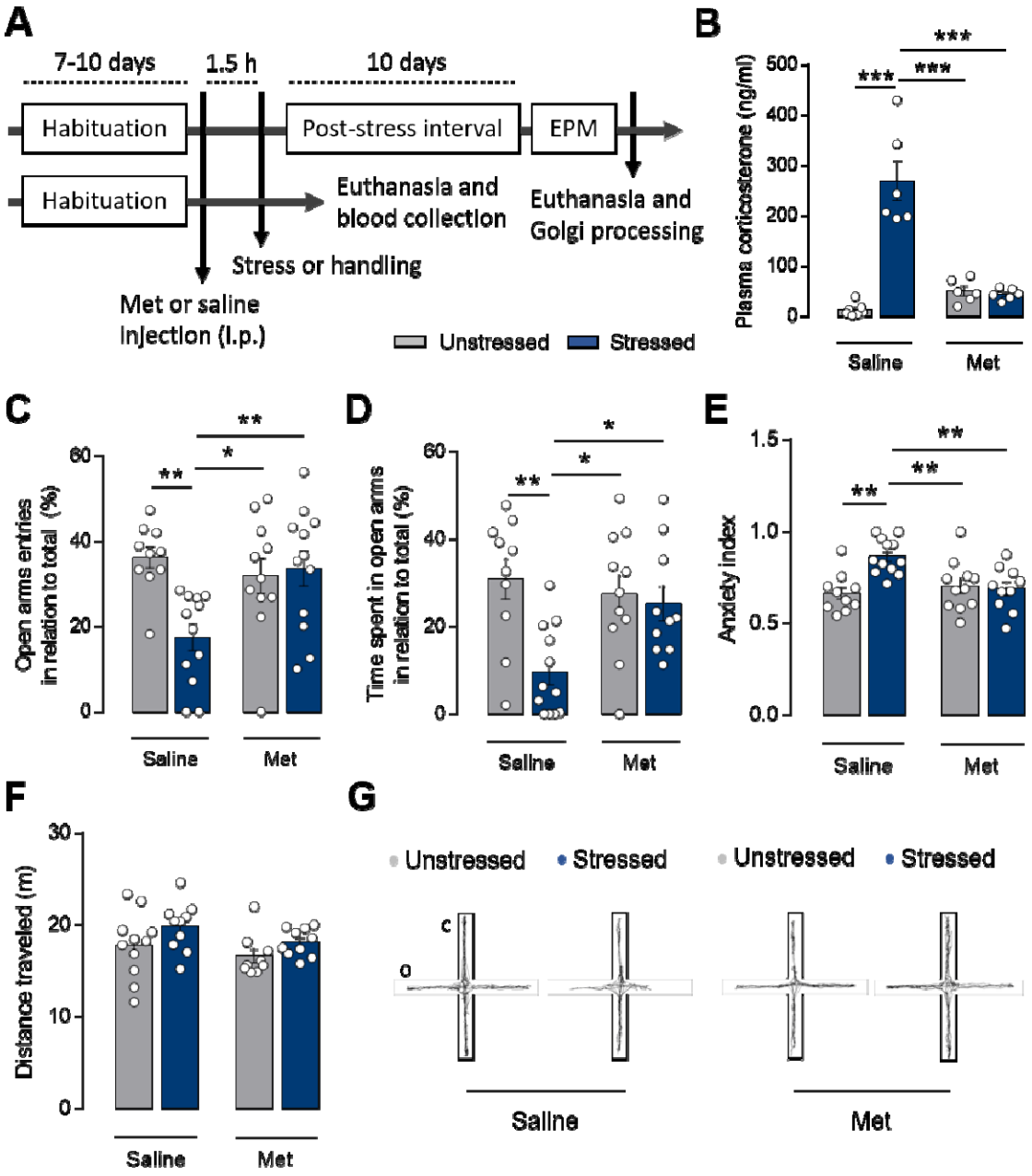

724

725 **Figure 1. CORT synthesis inhibition during stress prevented the delayed emergence**
726 **of anxiety-like behavior.** (A) Schematic representation of the experimental design
727 showing the timeline of vehicle (saline) or metyrapone (Met) injections, the stress
728 submission, and the EPM behavioral test. One cohort of animals was euthanized
729 immediately after the end of the stress session. (B) Previous administration of Met

730 prevented the stress-induced increase in CORT plasma levels measured immediately after
731 stress (n = 6–7 animals for each group, two-way ANOVA: stress $F_{1, 21} = 40.34$, $P < 0.0001$;
732 Met $F_{1, 21} = 22.81$, $P = 0.0001$; stress-Met interaction $F_{1, 21} = 44.35$, $P < 0.0001$). (C and D)
733 Stressed animals treated with saline exhibited reduced open arms entries (C; n = 10–12
734 animals for each group, two-way ANOVA: stress $F_{1, 40} = 4.692$, $P = 0.0363$; Met $F_{1, 40} =$
735 3.23, $P = 0.0799$; stress-Met interaction $F_{1, 40} = 8.9$, $P = 0.0048$) and time spent (D; n = 10–
736 12 animals for each group, two-way ANOVA: stress $F_{1, 39} = 8.712$, $P = 0.0053$; Met $F_{1, 39} =$
737 5.783, $P = 0.0210$; stress-Met interaction $F_{1, 39} = 2.352$, $P = 0.1332$) in the EPM test
738 compared to saline-treated non-stressed animals and to both stressed and non-stressed
739 Met-treated animals. (E) Stress increased the anxiety index in saline-treated but not in Met-
740 treated rats (n = 10–12 animals for each group, two-way ANOVA: stress $F_{1, 39} = 6.85$, $P =$
741 0.0126; Met $F_{1, 39} = 3.786$, $P = 0.0589$; stress-Met interaction $F_{1, 39} = 9.282$, $P = 0.0041$).
742 (F) Neither stress nor Met administration influenced the animal's locomotor activity in the
743 EPM (n = 9–12 animals for each group, two-way ANOVA: stress $F_{1, 34} = 2.388$, $P = 0.1315$;
744 Met $F_{1, 34} = 3.78$, $P = 0.0602$; stress-Met interaction $F_{1, 34} = 0.1839$, $P = 0.6707$). (G)
745 Representative tracking plots for the average motion of each experimental group in the
746 EPM. Results are represented as mean ± SEM. Tukey's multiple comparisons post-hoc test.
747 Significance differences between groups are indicated as * $P < 0.05$; ** $P < 0.01$; and *** $P <$
748 0.001.

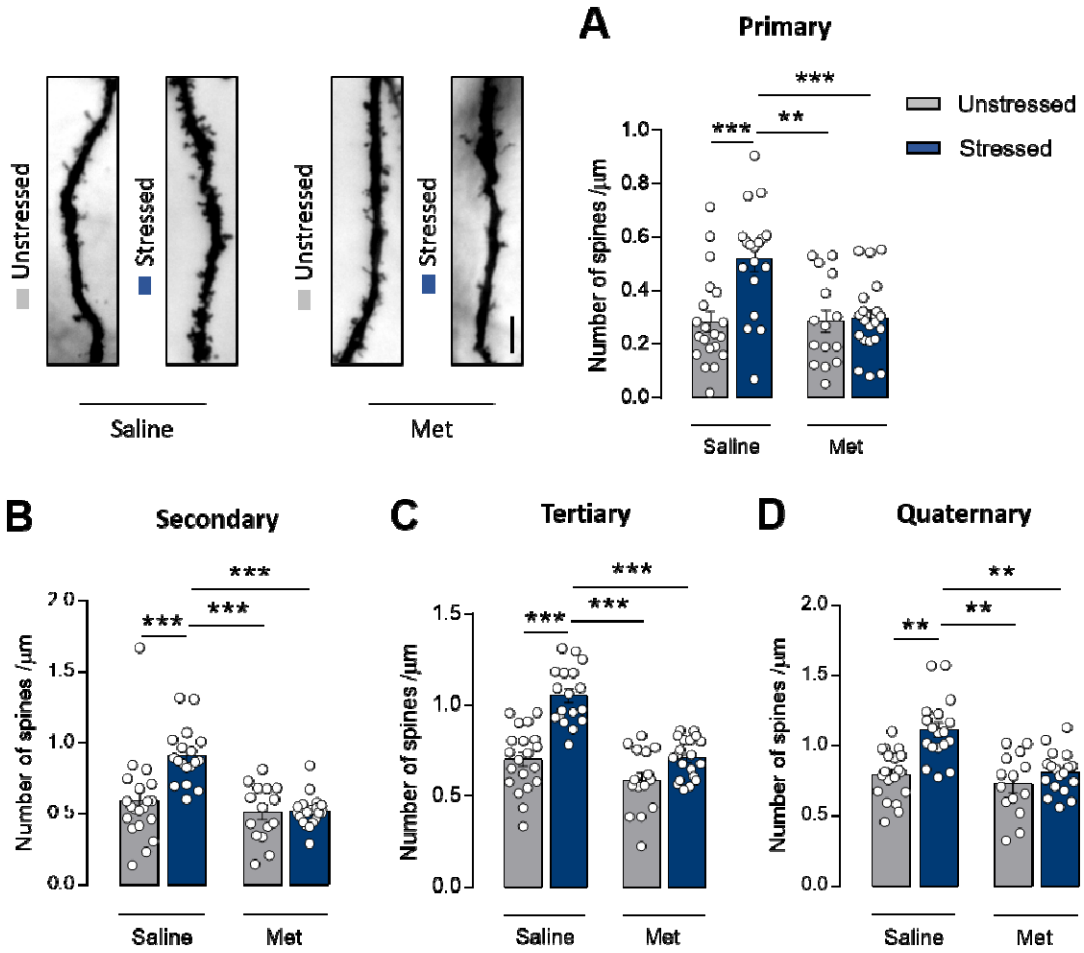

749

750 **Figure 2. Pre-stress Met administration prevented the stress-induced increase in BLA**
751 **dendritic spine density.** (A–D) Stressed saline-treated animals showed an increase in
752 spine density, effect prevented by pre-stress Met administration, in the primary (A; n = 15–
753 20 neurons for each group, two-way ANOVA: stress $F_{1, 69} = 9.351$, $P = 0.0032$; Met $F_{1, 69} =$
754 7.786, $P = 0.0079$; stress-Met interaction $F_{1, 69} = 7.72$, $P = 0.0070$), secondary (B; n = 15–20
755 neurons for each group, two-way ANOVA: stress $F_{1, 69} = 9.871$, $P = 0.0025$; Met $F_{1, 69} =$
756 20.65, $P < 0.0001$; stress-Met interaction $F_{1, 69} = 8.895$, $P = 0.0038$), tertiary (C; n = 15–20
757 neurons for each group, two-way ANOVA: stress $F_{1, 69} = 42.17$, $P < 0.0001$; Met $F_{1, 69} =$
758 39.75, $P < 0.0001$; stress-Met interaction $F_{1, 69} = 9.809$, $P = 0.0025$), and quaternary (D; n =
759 14–20 neurons for each group, two-way ANOVA: stress $F_{1, 65} = 18.62$, $P < 0.0001$; Met $F_{1,}$
760 $_{65} = 15.92$, $P = 0.0002$; stress-Met interaction $F_{1, 65} = 6.267$, $P = 0.0148$) dendrite segments
761 compared to non-stressed animals. (Top, left) Representative photomicrography of a BLA's
762 secondary dendrite segment. (Scale bar, 10 µm). Results are represented as mean ± SEM.

763 Tukey's multiple comparisons post-hoc test). Significance differences between groups are
764 indicated as ** $P < 0.01$ and *** $P < 0.001$.

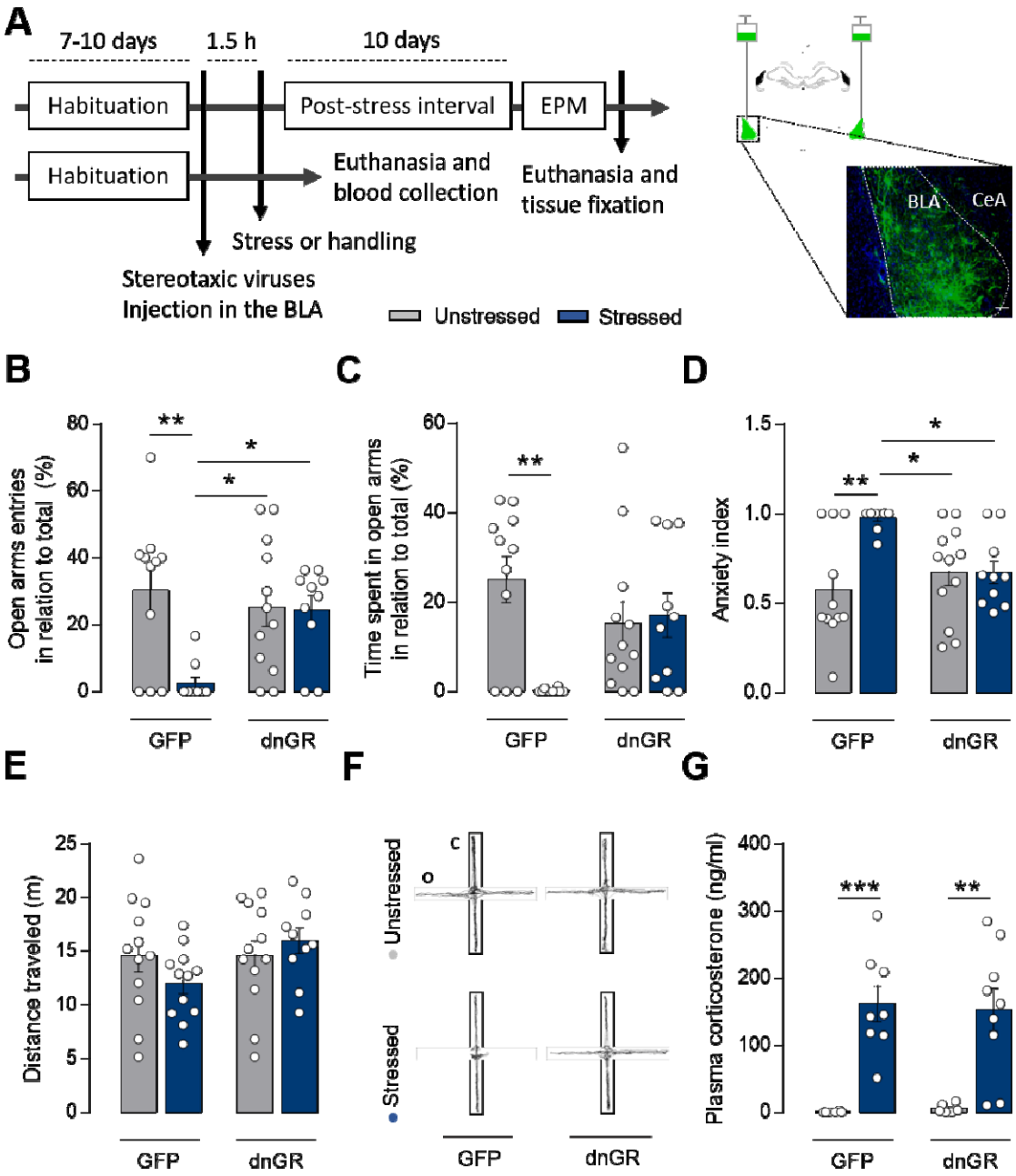

765

766 **Figure 3. dnGR overexpression in the BLA prevented the delayed emergence of stress-**
767 **induced anxiety-like behavior**. (A, left) Schematic representation of the experimental
768 design shows the virus injection timeline into BLA (GFP or dnGR), the stress submission,
769 and the EPM behavioral test. A cohort of animals was euthanized immediately after the end
770 of the stress session. (Right) Representative figure showing the viral injection into BLA and
771 photomicrography of an infected BLA (GFP, green). (Scale bar, 100 μm). CeA: central

772 nucleus of the amygdala. (B) GFP stressed animals exhibited reduced open arm entries in
773 the EPM test compared to GFP non-stressed animals and to both stressed and non-stressed
774 animals overexpressing dnGR in the BLA (n = 10–12 animals for each group, two-way
775 ANOVA: stress $F_{1, 39} = 7.527$, $P = 0.0091$; dnGR $F_{1, 39} = 2.612$, $P = 0.1114$; stress-dnGR
776 interaction $F_{1, 39} = 6.724$, $P = 0.0133$). (C) GFP stressed animals spent less time in the EPM
777 open arms compared to GFP non-stressed animals. dnGR animals (stressed and non-
778 stressed) exhibited no differences in time spent in open arms compared to GFP non-
779 stressed animals (n = 10–12 animals for each group, two-way ANOVA: stress $F_{1, 39} = 6.595$,
780 $P = 0.0142$; dnGR $F_{1, 39} = 0.6368$, $P = 0.4297$; stress-dnGR interaction $F_{1, 39} = 8.864$, $P =$
781 0.0050). (D) Stress increased the anxiety index in GFP-expressing but not in dnGR-
782 expressing rats (n = 10–12 animals for each group, two-way ANOVA: stress $F_{1, 39} = 7.943$, P
783 $= 0.0075$; dnGR $F_{1, 39} = 2.06$, $P = 0.1592$; stress-dnGR interaction $F_{1, 39} = 8.047$, $P =$
784 0.0072). (E) Neither stress nor BLA virus infection influenced the animal's locomotor
785 activity in the EPM (n = 10–12 animals for each group, two-way ANOVA: stress $F_{1, 42} =$
786 0.212, $P = 0.6476$; dnGR $F_{1, 42} = 2.257$, $P = 0.1405$; stress-dnGR interaction $F_{1, 42} = 2.283$,
787 $P = 0.1383$). (F) Representative tracking plots for the average motion of each experimental
788 group in the EPM. (G) Acute restraint stress promotes, immediately after the stressor
789 stimulus, an increase in CORT plasma levels in both GFP- and dnGR-overexpressing animals
790 (n = 6–9 animals for each group, two-way ANOVA: stress $F_{1, 25} = 36.25$, $P < 0.0001$; dnGR
791 $F_{1, 25} = 0.007222$, $P = 0.9330$; stress-dnGR interaction $F_{1, 25} = 0{,}07801$, $P = 0.7823$).
792 Results are represented as mean ± SEM. Tukey's multiple comparisons post-hoc test.
793 Significance differences between groups are indicated as * $P < 0.05$, ** $P < 0.01$, and *** $P <$
794 0.001.

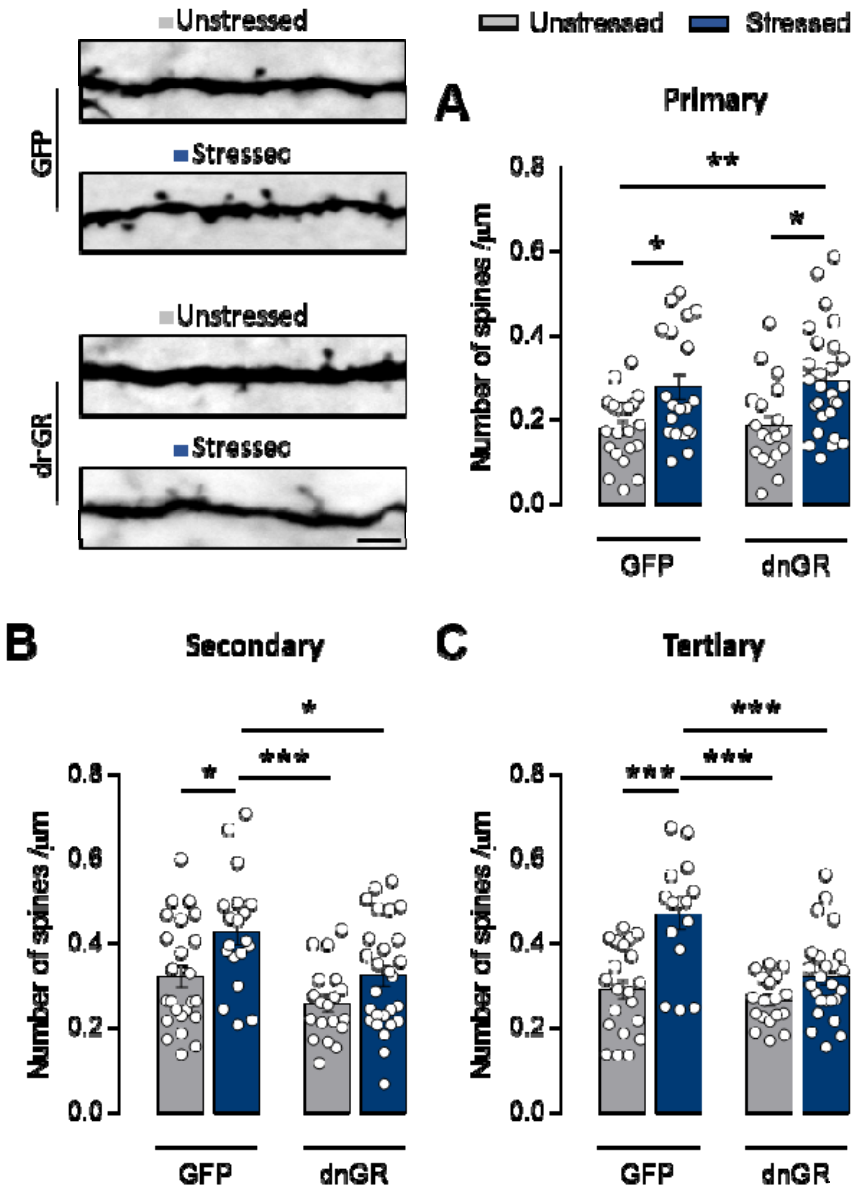

795

796 **Figure 4. dnGR expression in the BLA prevented the stress-related increase in BLA's**
797 **dendritic spine density.** (A–C) GFP stressed animals showed an increase in spine density,
798 effect prevented by the dnGR overexpressing in the BLA, in the primary (A; n = 19–27
799 neurons for each group, two-way ANOVA: stress $F_{1, 83} = 17.32$, $P < 0.0001$; dnGR $F_{1, 83} =$
800 0.188, $P = 0.6657$; stress-dnGR interaction $F_{1, 83} = 0.02408$, $P = 0.8771$), secondary (B; n =
801 19–27 neurons for each group, two-way ANOVA: stress $F_{1, 85} = 10.49$, $P = 0.0017$; dnGR $F_{1,}$
802 $85 = 10.34$, $P = 0.0018$; stress-dnGR interaction $F_{1, 85} = 0.6021$, $P = 0.4399$), and tertiary (C;
803 n = 15–25 neurons for each group, two-way ANOVA: stress $F_{1, 69} = 16.8$, $P = 0.0001$; dnGR

804 F1, 69 = 8.421, P = 0.0050; stress-dnGR interaction F1, 69 = 7.85, P = 0.0066) dendrite
805 segments compared to non-stressed animals. (Top, left) Representative photomicrography
806 of a BLA's secondary dendrite segment. (Scale bar, 10 μm). Results are represented as mean
807 ± SEM. Tukey's multiple comparisons post-hoc test. Significance differences between groups
808 are indicated as * P < 0.05, ** P < 0.01, and *** P < 0.001.

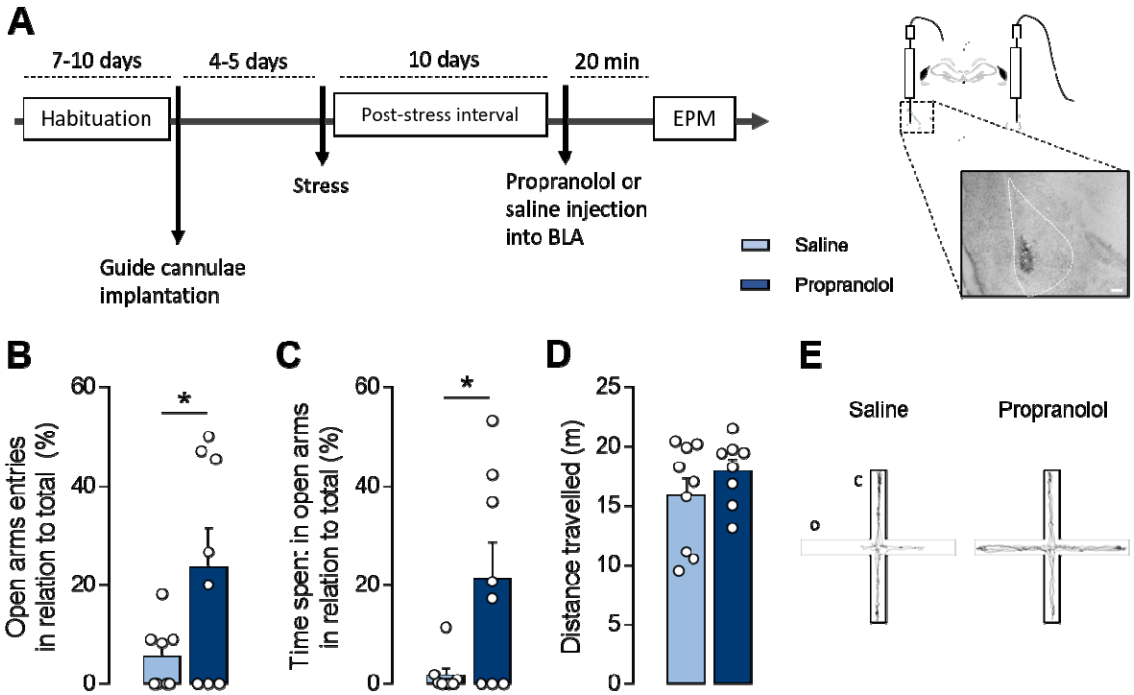

Figure 5. Pre-EPM test propranolol administration in the BLA prevented the delayed manifestation of the stress-induced anxiety-like behavior. (A, left) Schematic representation of the experimental design shows the propranolol or saline injection timeline into BLA, the stress submission, and the EPM test. (Right) Representative figure and photomicrography showing a representative location of cannulae and injection needle tips into BLA. (B–E) Stressed, intra-BLA saline administered animals exhibited reduced open arms entries (B; n = 8 animals per group, two-tailed Student's t-test: P = 0.0441) and time spent (C; n = 8 animals per group, two-tailed Student's t-test: P = 0.0218) in the EPM test comparing to stressed, intra-BLA propranolol administered animals. (D) There was no influence of intra-BLA propranolol administration on the animal's locomotor activity in the EPM (n = 8-9 animals per group, two-tailed Student's t-test: P = 0.0285). (E) Representative tracking plots for the average motion of each experimental group in the EPM. Results are represented as mean ± SEM. Significance differences between groups are indicated as * P < 0.05.

825 **Supplementary Figures and Tables**

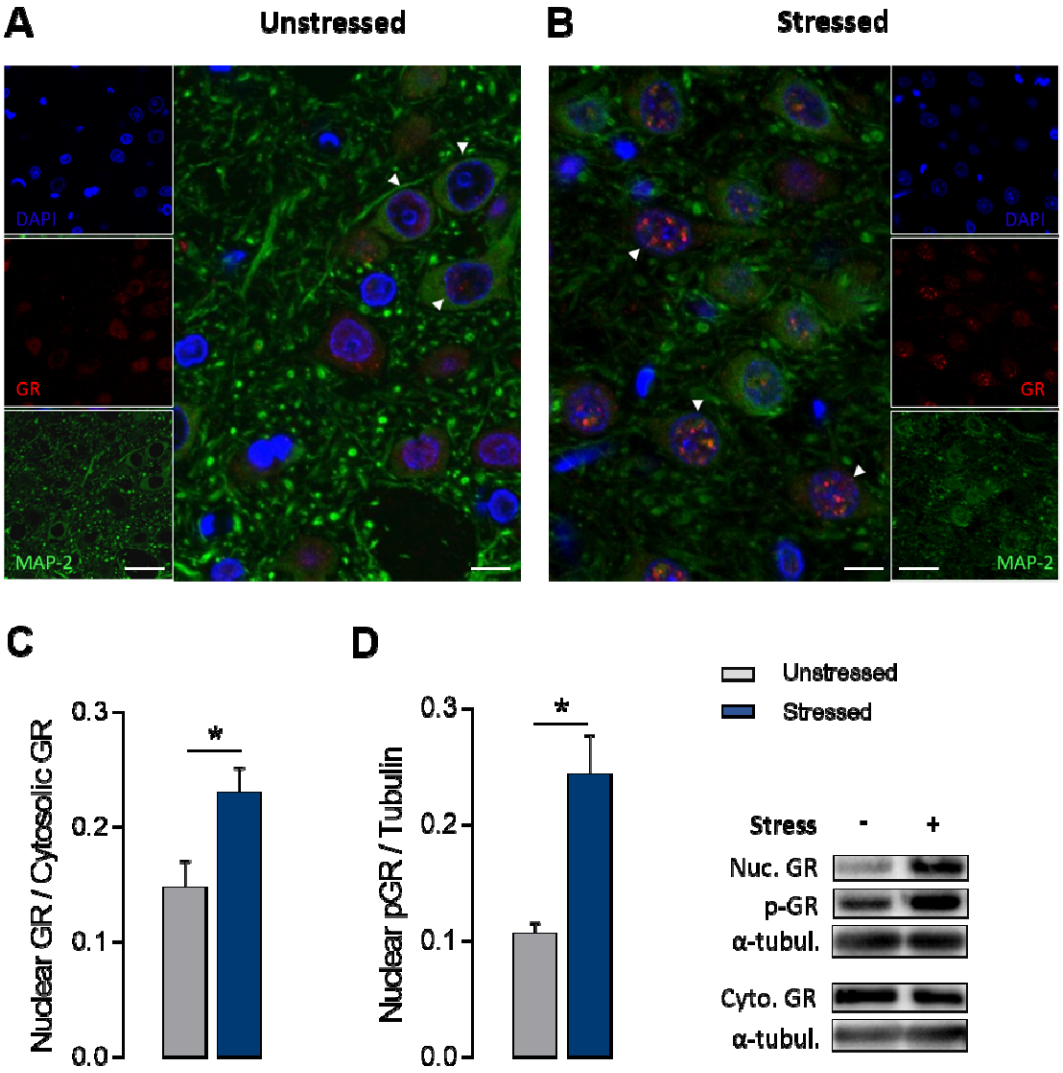

826

827

828 **Figure S1**. Acute restraint stress affects GR nuclear translocation and GRser211
829 phosphorylation in the BLA. (A and B) BLA immunofluorescence showing increased
830 accumulation of GR (red) in the nucleus of neurons (green, MAP-2) from stressed animals
831 (B) compared to non-stressed animals immediately after the cessation of stress (A). DAPI
832 (blue) was used as a nuclear marker. Arrowheads indicate the nuclear region of neurons.
833 (Scale bars on smaller and larger panels correspond to 25 μm and 8 μm, respectively).
834 Images were acquired in a confocal microscope sectioned in the Z plane at 0.6 μm. (C and D)
835 Western blot analysis showed an increase in GR nuclear translocation (C; n = 4-5 for each

836 group, two-tailed student´s t-test: P = 0.0346), as well as in GRser211 phosphorylation (D; n
837 = 3 for each group, two-tailed student´s t-test: P = 0.0166) in stressed animals compared to
838 unstressed ones. (Bottom, right) Representative autoradiography of Western blot. Results
839 are represented as mean ± SEM. Significance differences between groups are indicated as *
840 P < 0.05.

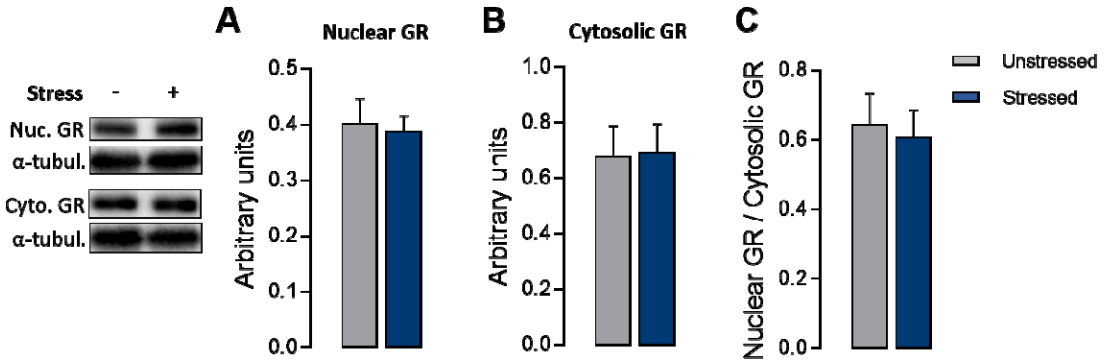

Figure S2. GR expression in the BLA 10 days after the stress. Acute restraint stress has no delayed effect on GR nuclear translocation in the BLA. (Left) Representative autoradiography of Western blot. (A–C) Western blot analysis showed no effect of stress on nuclear GR (A; n = 5 per group, two-tailed student´s t-test: P = 0.7837), cytosolic GR (B; n = 5 per group, two-tailed student´s t-test: P = 0.9408), or the nuclear-cytosolic ratio (C; n = 5 per group, two-tailed student´s t-test: P = 0.7571). Results are represented as mean ± SEM.

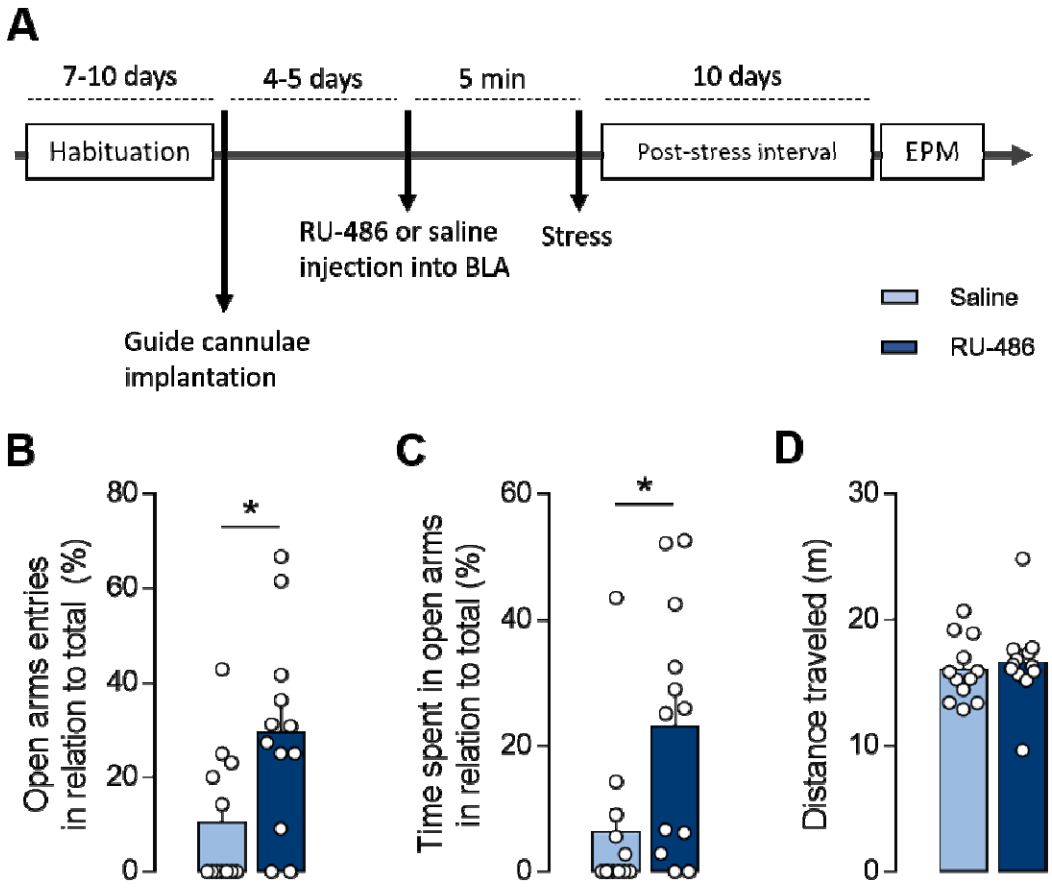

Figure S3. Pre-stress intra-BLA GR antagonist RU-486 administration prevented the delayed emergence of stress-induced anxiety-like behavior. (A) Schematic representation of the experimental design showing the timeline of RU-486 or saline injection into BLA, the stress submission, and the EPM behavioral test. (B–D) Pre-stress intra-BLA saline administered animals exhibited reduced open arms entries (B; n = 12 animals per group, two-tailed student's t-test: P = 0.0161) and time spent (C; n = 12 animals per group, two-tailed student's t-test: P = 0.0215) in the EPM test comparing to RU-486 administered animals. (D) There was no influence of intra-BLA RU-486 administration on the animal's locomotor activity in the EPM (n = 12 animals per group, two-tailed student's t-test: P = 0.6168). Results are represented as mean ± SEM. Significance differences between groups are indicated as * P < 0.05.

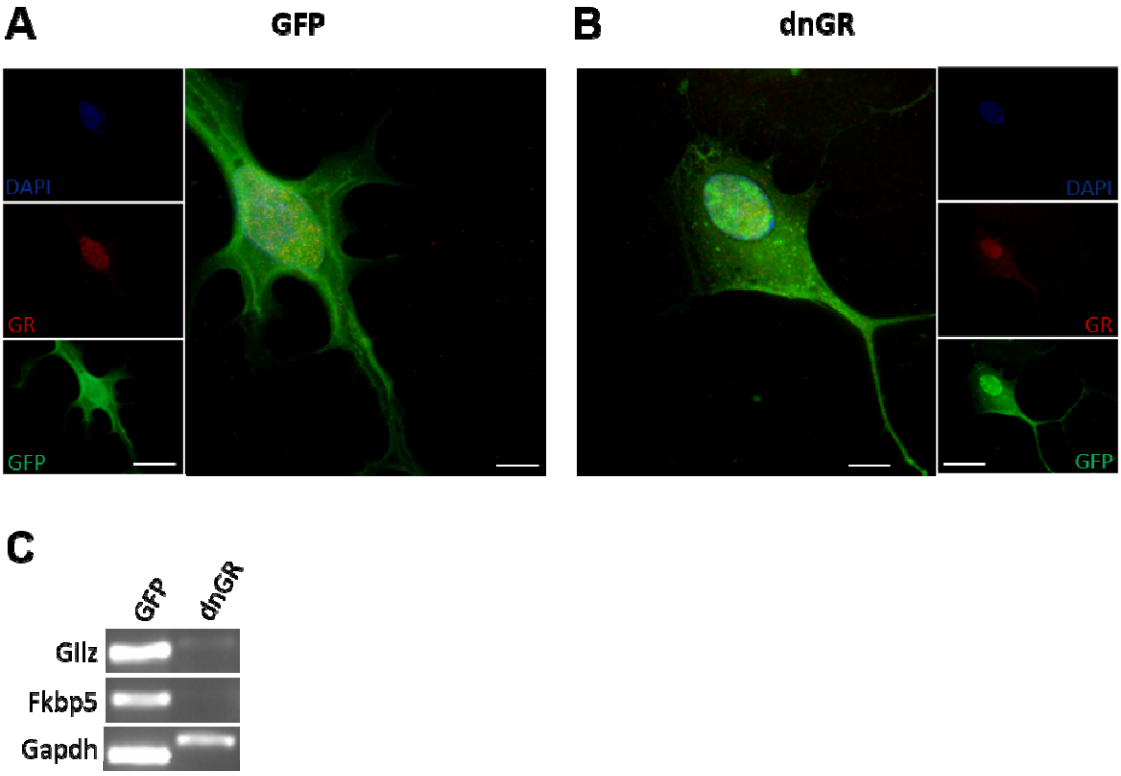

Figure S4. dnGR- and GFP-infected cells response to the challenge with CORT. (A and B) Primary culture immunofluorescence of rat cortex showing GR (red) distribution in the cytoplasmic and nuclear compartments of neurons. Neurons were infected with GFP (A) or dnGR (B) and stimulated with CORT (10 µM, 1h). DAPI was used as a nuclear marker (Blue), and GFP is represented in green. (Scale bars on smaller and larger panels correspond to 30 µm and 10 µm, respectively). (C) RT-PCR cDNA amplicons for GILZ, FKBP5, and GAPDH in GFP- and dnGR-infected cells treated with CORT (10 µM, 1h).

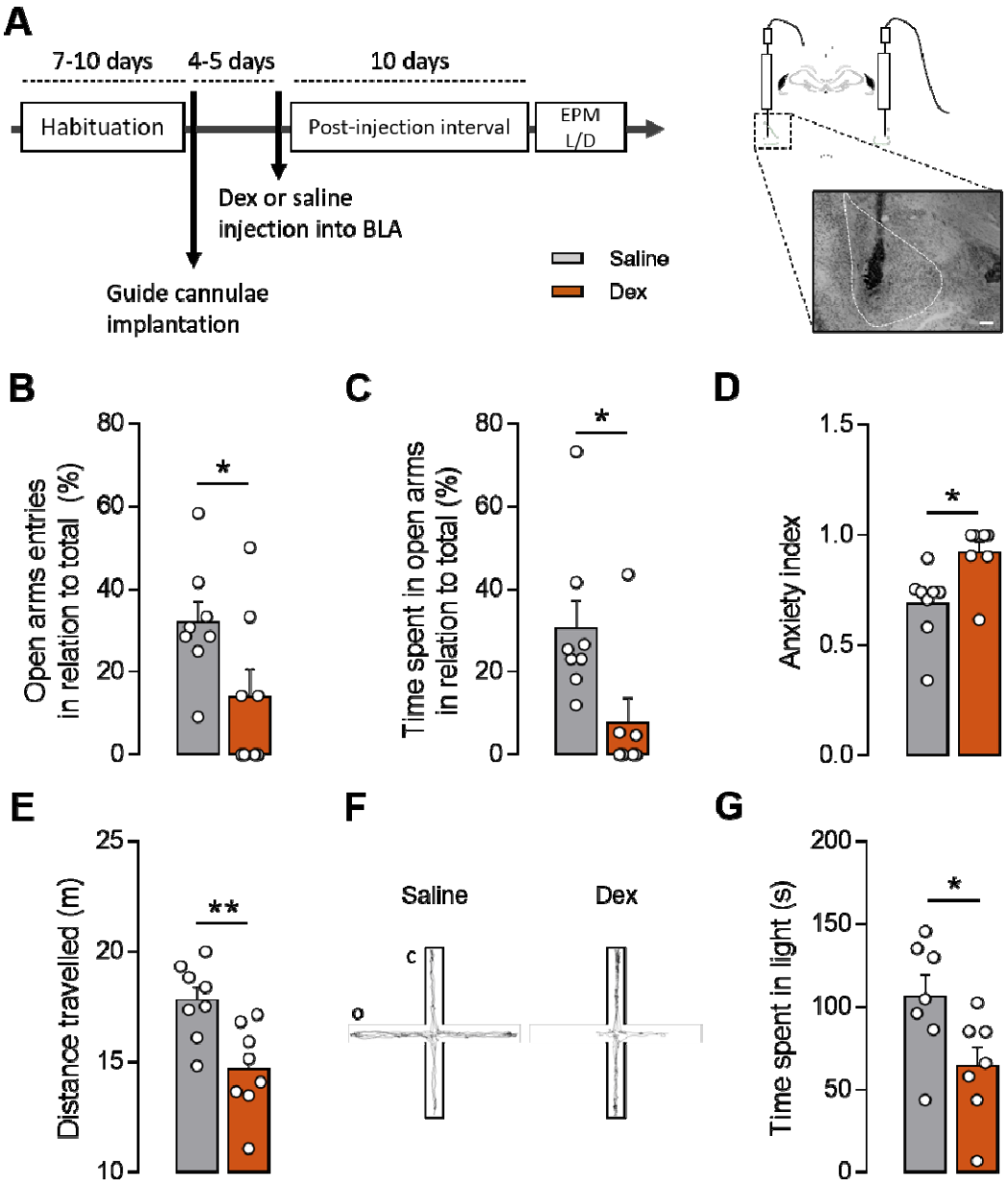

Figure S5. Intra-BLA dexamethasone administration promotes an anxiety-like behavior ten days after infusion. (A, left) Schematic representation of the experimental design showing the timeline of dexamethasone (Dex) or saline injection into BLA, the stress submission, and the behavioral tests. (Right) Representative figure and photomicrography showing a representative location of cannulae and injection needle tips into BLA. (Scale bar, 100 µm); (B–D) Intra-BLA dexamethasone administered animals exhibited reduced open arms

879 entries (B; n = 8 animals per group, two-tailed student´s t-test: P = 0.0482) and time spent
880 (C; n = 7-8 animals per group, two-tailed student´s t-test: P = 0.0285), as well as increased
881 anxiety index (D; n = 7-8 animals per group, two-tailed student´s t-test: P = 0.0127) in the
882 EPM test comparing to saline administered animals. (E) Intra-BLA dexamethasone
883 promoted a delayed reduced motor activity in the EPM test (n = 8 animals per group, two-
884 tailed student's t-test: P = 0.0048). (F) Intra-BLA dexamethasone administration promoted
885 a delayed decrease in time spent in the lit compartment compared to saline administered
886 animals in the light/dark (L/D) test (n = 7 animals per group, two-tailed student's t-test: P =
887 0.0369). (G) Representative tracking plots for the average motion of each experimental
888 group in the EPM. Results are represented as mean ± SEM. Significance differences between
889 groups are indicated as * P < 0.05.

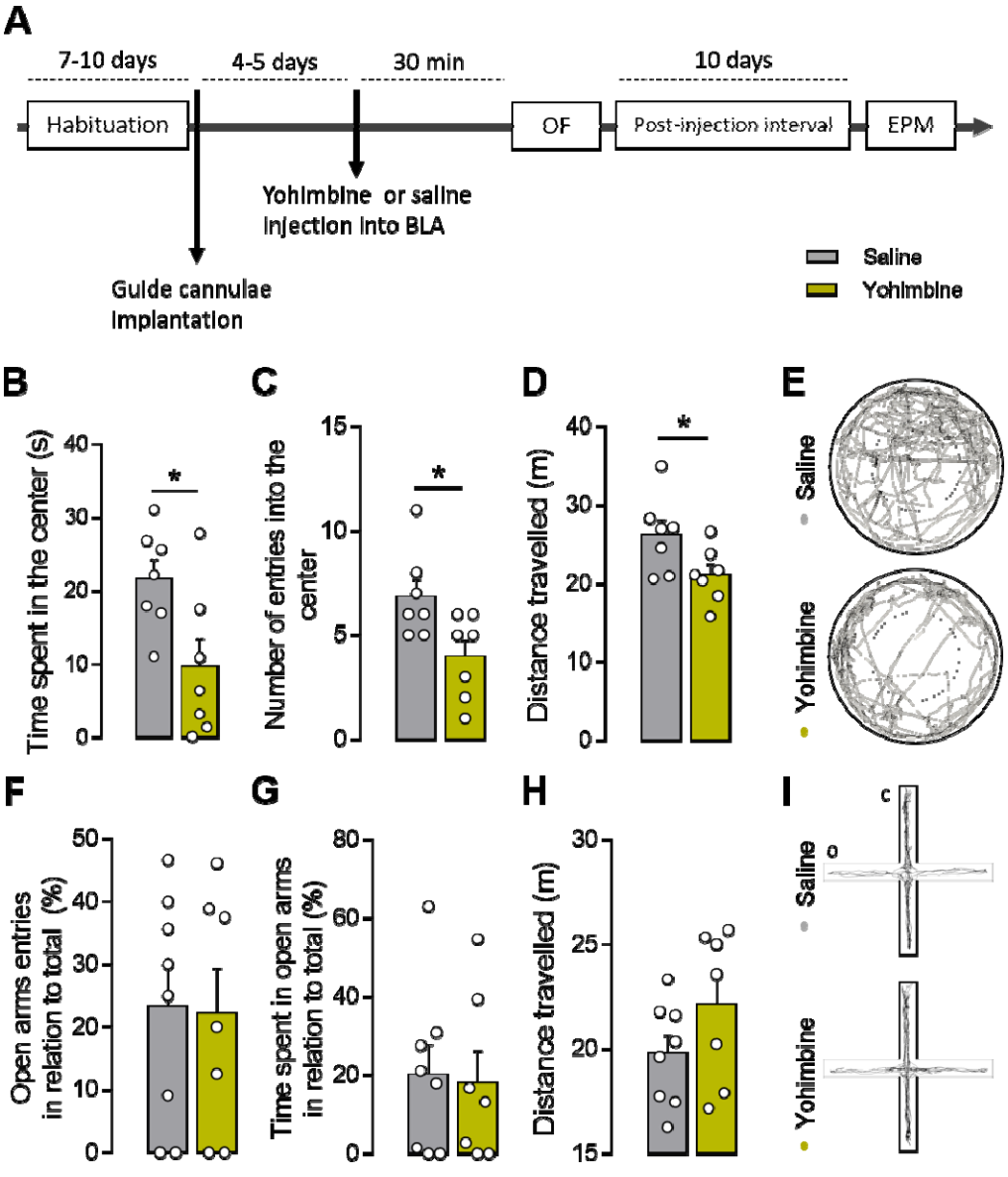

Figure S6. Intra-BLA yohimbine administration promotes an acute, but not delayed, anxiety-like behavior. (A, left) Schematic representation of the experimental design showing the timeline of yohimbine or saline injection into BLA and the behavioral tests. (Right) Representative figure and photomicrography showing a representative location of cannulae and injection needle tips in the BLA. (B-C) Animals that received intra-BLA yohimbine exhibited reduced time spent (B; n = 7 animals per group, two-tailed student's t-test: P = 0.0225) and entries (C; n = 7 animals per group, two-tailed student's t-test: P = 0.0234) in

899 the center area of the OF. (D) Intra-BLA yohimbine promoted an acute decrease in motor
900 activity in the OF (n = 7 animals per group, two-tailed student's t-test: P = 0.00462). (E)
901 Representative tracking plots for the average motion of each experimental group in the OF.
902 (F-G) There were no differences in the open arms entries (F; n = 7-8 animals per group,
903 two-tailed student's t-test: P = 0.9058) and time spent (G; n = 7-8 animals per group, two-
904 tailed student's t-test: P = 0.8491) in the EPM test of BLA yohimbine administered animals
905 comparing to saline administered animals. (H) Intra-BLA yohimbine did not influence the
906 animal's locomotor activity in the EPM (n = 7-8 animals per group, two-tailed student's t-
907 test: P = 0.1617). (I) Representative tracking plots for the average motion of each
908 experimental group in the EPM. Results are represented as mean ± SEM. Significance
909 differences between groups are indicated as * P < 0.05.